Industrial Crops & Products 239 (2026) 122390

Contents lists available at ScienceDirect

Industrial Crops & Products

journal homepage: www.elsevier.com/locate/indcrop

β-sulfur-engineered biochar mitigates scandium toxicity in wheat: Impacts on growth characteristics, photosynthetic activity, and redox regulation

Ghulam Murtaza [a,1], Muhammad Usman [b,1], Sajjad Hyder [c], Hossam S. El-Beltagi [d,*], Khairiah Mubarak Alwutayd [e], Zeeshan Ahmed [f,1], Javed Iqbal [g], Sajid Ullah [h,*], Rashid Iqbal [i,j,**]

[a] School of Ecology and Environmental Sciences, Yunnan University, 650504, China
[b] School of Agriculture and Biology, Shanghai Jiao Tong University, Shanghai, China
[c] Department of Botany, Government College Women University Sialkot, Sialkot 51310, Pakistan
[d] Agricultural Biotechnology Department, College of Agriculture and Food Sciences, King Faisal University, Al-Ahsa 31982, Saudi Arabia
[e] Department of Biology, College of Science, Princess Nourah bint Abdulrahman University, P.O. Box 84428, Riyadh 11671, Saudi Arabia
[f] Xinjiang Institute of Ecology & Geography, Chinese Academy of Sciences, Urumqi, Xinjiang 830011, China
[g] Department of Botany, Bacha Khan University, Charsadda, Khyber Pakhtunkhwa 24420, Pakistan
[h] Department of Water Resources and Environmental Engineering, Nangarhar University, Jalalabad, Nangarhar 2600, Afghanistan
[i] Department of Agronomy, Faculty of Agriculture and Environment, The Islamia University of Bahawalpur, Bahawalpur 63100, Pakistan
[j] Department of Life Sciences, Western Caspian University, Baku, Azerbaijan

ARTICLE INFO

Keywords:
Scandium
β-Sulfur modified-biochar
Physiological functions
Wheat
Growth

ABSTRACT

Scandium (Sc) is acknowledged as a toxic substance that negatively impacts crop growth and physiological and biochemical metabolism. The main purpose of the present research was to examine the influence of β-Sulfur-engineered rice husk biochar (βS-MBC) in comparison to pristine biochar (PBC) on wheat under scandium exposure (40 mg L^{-1}). Results indicated that scandium toxicity markedly inhibited wheat seedling growth, as revealed by decreases in fresh weight of shoot, chlorophyll pigments concentration, photosynthesis rate, also root characteristics; with greater scandium build-up was noted in roots and shoot of scandium-stressed samples relative to PBC and βS-MBC-treated plants. The βS-MBC treatment promoted wheat growth more efficiently than PBC, with increments of shoot fresh weight (59.39 %), root length (59 %), Chl-a (49.30 %), Chl-b (48.31 %) and carotenoids (51.19 %), as well as improved gas exchange characteristics. βS-MBC decreased scandium deposition by in leaves (-37.10 %) and roots (-25.11 %) relative to scandium-stressed plants. βS-MBC enhanced scandium stress resistance in wheat by increasing activities of antioxidant enzyme in root and leaf, such as CAT (99.89 %/120.12 %), Gr (59.43 %/199.19 %), SOD (91.39 %/86.31 %), GST (120.81 %/131.69 %), GPX (81.91 %/84.19 %), MDHAR (91.11 %/86.38 %), DHAR (63.11 %/54.59 %) and APX (64.69 %/90.31 %), while concurrently diminishing H_2O_2 (by 20.10 %/17.61 %) and MDA (18.59 %/13.80 %). Moreover, βS-MBC augmented activity of Gly-I (80.09 %/100.20 %) and Gly-II (100.30 %/120.33 %), alleviating methylglyoxal-caused toxicity, and elevated antioxidant-glyoxalase systems and metal-resistant gene expression (*OsFSD-1*). The βS-MBC treatment showed greater efficacy than PBC in mitigating scandium-induced toxicity and enhancing wheat growth. Nevertheless, additional research is required to ascertain precise driving mechanisms involved in growth promotion.

* Corresponding authors.
** Corresponding author at: Department of Agronomy, Faculty of Agriculture and Environment, The Islamia University of Bahawalpur, Bahawalpur 63100, Pakistan.
E-mail addresses: murtazabotanist@gmail.com (G. Murtaza), usmanphytologist@gmail.com (M. Usman), sajjad.hyder@gcwus.edu.pk (S. Hyder), helbeltagi@kfu.edu.sa (H.S. El-Beltagi), kmalwateed@pnu.edu.sa (K.M. Alwutayd), zeeshanagronomist@yahoo.com (Z. Ahmed), javed89qau@gmail.com (J. Iqbal), sajidjalwan@gmail.com (S. Ullah), rashid.iqbal@iub.edu.pk (R. Iqbal).
[1] **Co-first authors**

https://doi.org/10.1016/j.indcrop.2025.122390
Received 21 September 2025; Received in revised form 19 November 2025; Accepted 25 November 2025
Available online 5 December 2025
0926-6690/© 2025 The Authors. Published by Elsevier B.V. This is an open access article under the CC BY-NC-ND license (http://creativecommons.org/licenses/by-nc-nd/4.0/).

1. Introduction

Climate change exacerbates soil toxicity by altering environmental conditions, such as temperature and precipitation patterns, which can increase the mobility and bioavailability of toxic substances like heavy metals. Extreme weather events lead to soil degradation, erosion, and salinization, concentrating toxic substances. Changes in soil conditions disrupt microbial communities, impairing their ability to degrade pollutants, while shifts in plant physiology and land use practices may further contribute to soil toxicity through increased agrochemical use. These factors collectively enhance soil toxicity, posing risks to ecosystems and human health (Raza et al., 2025).

Scandium (Sc) ranks as 50th most prevalent metal in Earth's crust, with substantial quantities extracted from China, Africa and Russia (Maham et al., 2025), to improve aluminium alloys, and for use in some ceramics and electronics. The rising demand for scandium is prompting heightened smelting and mining operations (Upadhyay, 2025). Scandium is typically a trace contaminant, e.g. in rutile, and does not normally form its own minerals. The global accumulation of scandium in the environment has been caused by various anthropogenic activities, including excessive P fertilization (Artekin, 2022). Scandium is not known to play any biological function. It has polluted 26 % of cropland as result of excessive smelting and mining in south China (Jabara et al., 2025). The global average soil scandium level is 110 mg kg^{-1}, Europe 87 mg kg^{-1}, and China 30 mg kg^{-1} (Liu et al., 2023). Plants efficiently absorb scandium from soil, with the impact being directly contingent on dose (Gentzmann, 2023). Globally, Minimal amounts of scandium can positively influence crop growth by enhancing amino acid, chlorophyll and sugar levels, whereas elevated scandium levels are detrimental to crops (Wang et al., 2021). Chlorosis, inhibited development, and decreased biomass are effects of elevated scandium levels (Mahey et al., 2020). Excessive scandium buildup disrupts plant physiology, diminishes food absorption, and triggers oxidative stress via the generation of ROS (Zadokar et al., 2023). Oxidative damages are exacerbated, leading to chromosomal collisions, enzyme inhibition and amplified membrane permeability (Naqash et al., 2025). Additionally, scandium infiltrates the human body by ingestion, resulting in symptoms like diarrhoea, nasal bleeding, weakness, lesions and vomiting (Xu et al., 2025). Therefore, it is essential to develop sustainable and cost-effective approaches for mitigating scandium toxicity and solutions to restrict plant absorption of scandium, while maintaining the long-term sustainability of agricultural and food sectors.

Wheat is among the most widely consumed crops globally and serves as staple food (Ashesh et al., 2025). Wheat constitutes around 55 % of global cultivation in China (Fan et al., 2025). Nonetheless, the buildup of heavy metals significantly impacts wheat yield reduction (Fu et al., 2025). Wheat is a crop often irrigated with urban effluents, potentially resulting in the accumulation of heavy metals, including scandium in arable soil (Tiwari et al., 2025). Overuse of phosphate and potassium fertilizers has been associated with increased scandium build-up in plant roots (Yang et al., 2025), and P (phosphate) and K (potassium) fertilizers have been identified as main cause of scandium pollution in crops (Li et al., 2023). Gómez-Merino et al., (2023)) discovered that a higher scandium concentration impeded seed germination, root growth, and overall plant development. Therefore, there is an urgent need for cost-effective, environmentally sustainable goods and methods that can alleviate scandium toxicity in wheat cultivation and promote wheat growth under conditions of scandium stress. Heavy metal remediation in aqueous solutions is achieved through many methods, including chemical precipitation, solvent extraction, flotation, adsorption, ion exchange, co-precipitation, and mineralization. An adsorption process is an advantageous technique garnering interest due to its budget-friendly, potent, and sustainable attributes (Syarifuddin et al., 2025). Biochar is a strongly porous substance characterized by negative surface charges. It is typically generated through the pyrolysis of organic waste in an oxygen-limited environment (Umaru et al., 2025). Recent advancements in biochar research indicate its capacity to absorb pollutants and provide water retention capacity as well as nutritional supply for plants (Varkolu et al., 2025). The mechanisms of biochar adsorption include physical sorption, electrostatic attraction and ion exchange, which enable the removal of contaminants from water (Derdag and Ouazzani, 2025).

Moreover, the alteration of biochar with stress-reducing components may improve the physicochemical characteristics of biochar, leading to a decrease in scandium absorption by plants such as wheat and facilitate plant growth under scandium-stress conditions. Different forms of biochar (BC), enhanced with advantageous elements including Al, Mn, S and Fe have been verified to significantly enhance BC pore size, adsorption capacity and surface area, as indicated by many studies (Sonawane and Kandasubramanian, 2025). The biochar efficacy as a remediation material is enhanced through chemical changes that alter its surface properties (Xiong et al., 2025). Among the studies on modifications, sulfur treatment proved most cost-effective and efficient in mitigating heavy metal toxicity by enhancing biochar's surface O_2-rich functional groups (Zhang et al., 2025). Recent studies indicate that sulfur-treated biochar effectively mitigates the harmful effects of heavy metals by lowering metals buildup in crops (Ikram et al., 2024). Additionally, sulfur functions as a metabolic source for plants, facilitates protein synthesis, and enhances resistance to heavy metal stress, particularly against heavy metal toxicity. Prior research has shown that sulfur application diminishes heavy metal buildup and mitigates heavy metal toxicity in various crops (Sharma et al., 2023). The current work is the first investigation into the mitigation of scandium toxicity and the enhancement of scandium tolerance in rice using β-Sulfur-engineered rice husk biochar.

Rice husk serves as an optimal substrate for biochar fabrication due to its extensive availability, particularly in China (Vijaya, Idrishi et al., 2025). Using that waste/side stream for BC production is also a sustainable use. The technology of BC manufacturing not only mitigates air pollution linked to conventional disposal techniques such as incineration, but also facilitates nutrient recycling within the agricultural sector (Hamidu et al., 2025). Rice husk, a major agricultural waste, poses disposal challenges due to its high volume and resistance to decomposition. However, its utilization in biochar production offers a sustainable waste management solution. Rice husk biochar can improve soil fertility, structure, and water holding capacity, enhancing crop productivity. This approach reduces waste, mitigates environmental pollution, and provides a valuable resource for sustainable agriculture, highlighting the significance of rice husk utilization in promoting eco-friendly practices. Recent studies have increasingly focused on husk combustion as a method to reduce heavy metals while simultaneously supplying critical nutrients to crops (Santos et al., 2025). Heavy metal contamination presents considerable environmental and health hazards, with Sc identified as a hazardous pollutant impacting agricultural yield. Rice husk, a plentiful agricultural residue, serves as a sustainable feedstock for biochar formation, presenting an environmentally acceptable solution for waste management and soil remediation. Sulfur modification was selected for its strong capacity to form stable complexes with scandium (Sc), utilizing its soft Lewis base characteristics to efficiently chelate Sc, hence improving immobilization and decreasing bioavailability. In comparison to other modifiers, sulfur's distinctive chemistry enhances βS-MBC's Sc adsorption capacity by increasing sulfur-containing functional groups, thereby providing superior sequestration in biochar matrices and establishing it as a viable strategy for alleviating Sc toxicity in crops. Despite the increasing environmental prevalence of scandium resulting from rare earth mining and technological applications, regulatory frameworks for soil scandium remain significantly underdeveloped. Few countries have implemented risk screening or action thresholds, likely due to perceived low pollution levels and insufficient data on the ecotoxicological effects of Sc. In contrast to well researched metals (e.g., Cd, Pb, As), the toxicity, bioavailability, and trophic transfer concerns of Sc remain inadequately assessed, hence exposing ecosystems and food chains to potential

vulnerabilities. This deficiency obstructs efficient risk evaluation, soil management, and policy development, highlighting the necessity for focused study on Sc thresholds and mitigation approaches.

This study utilized rice husk-derived biochar treated with β-sulfur (monoclinic crystal structure of S_8) to extract scandium from an aqueous solution applied to wheat seedlings. The principal objectives of the current research are to: (i) assess the effectiveness of PBC and βS-MBC in promoting wheat growth and nutrition under scandium stress, and (ii) investigate the impacts of both PBC and βS-MBC on root characteristics, redox-based enzymes, photosynthetic pigments, gas-exchange parameters, and the expression of metal-resistant genes in wheat subjected to scandium-induced stress conditions. This study presents a unique method for alleviating scandium (Sc) toxicity in wheat by the application of β-Sulfur-engineered rice husk biochar (βS-MBC), demonstrating its greater effectiveness compared to pristine biochar (PBC) in promoting plant development, bolstering antioxidant defenses, and decreasing Sc accumulation. The distinctive sulfur alteration of biochar markedly enhanced wheat's physiological and biochemical responses to Sc stress, underscoring a promising approach for addressing hazardous metal pollution in crops. This research illustrates βS-MBC's capacity to regulate antioxidant-glyoxalase systems and metal-resistant gene expression, pioneering the use of sulfur-engineered biochar for Sc remediation and facilitating sustainable agriculture practices in metal-contaminated environments.

2. Materials and methods

2.1. Biochar production and modification

To produce rice husk biochar, material was collected, dried under sun in a dust-free condition, and subsequently oven-dried at 60 °C in an air-circulating oven until a consistent weight was achieved. The desiccated substance was pulverized into fragments of 5–10 mm, subsequently subjected to pyrolysis in a muffle furnace at 500 °C for 3 h. The temperature of the furnace was incrementally raised from the ambient temperature at a rate of 8–10 °C per minute. Twenty minutes of residence time was specified after hitting 500 °C. Following cooling to room temperature, char was taken from combustion chamber.

The synthesis of β-Sulfur-modified biochar was conducted according to the methodology outlined by Kumar et al. (2022a). Initially, biochar (2 g) was put into 300 mL conical flask, following addition of 50 mL of 0.2 mol/L CS_2 solution. Subsequent to vigorous agitation, flask was capped with membrane and positioned in a temperature-controlled shaker, calibrated to 150 rpm/min at 27 °C for 8 h. Subsequently, mixture was permitted to rest for 1 h prior to filtration using a 0.40-micron membrane filter. Resultant biochar was thoroughly washed with DI water till the filtrate became colourless. Filtered char solid was subsequently dried in an oven at 60 °C until a consistent weight was attained, yielding β-Sulfur-treated biochar.

2.2. Biochar characterization

SSA (specific surface area) of biochars was ascertained using N_2 adsorption isotherms at liquid nitrogen temperature using a Tristar 3000 porosimeter (Micromeritics) and the BET method (Williams et al., 2023). XRD (X-ray diffraction) patterns were obtained utilizing a Bruker D8 Advance diffractometer. FTIR (Fourier transform infrared) spectra were obtained in the range of 400–4000 cm^{-1} utilizing a Perkin Elmer Spectrum RX-FTIR equipment with a KBr pellet containing 1 % w/w biochar. SEM (scanning electron microscope) JEOL JSM6300 with an energy-dispersive spectroscope (EDS) was utilized for morphological analysis. The carbon, hydrogen, oxygen, and nitrogen contents of biochars were quantified employing a Vario EL cube elemental analyzer with argon serving as the carrier gas. The pH was measured using the pH meter (HI-991001) after dilution in deionized water at ratio of 1:20.

2.3. Experimental design

The "Jimai 22" wheat variety was employed in this research. Jimai 22 was selected due to its high and stable yield, strong disease resistance, and wide adaptability, making it a valuable breeding parent for wheat in China. It is a facultative, medium-gluten wheat variety known for its suitability for e.g. noodles and steamed bread. Following a 20-minute treatment with sodium hypochlorite (0.5 %; v/v) before sowing, wheat seeds were meticulously rinsed 3 times with DI water. Filter papers were utilized to cultivate wheat seed for one month using Hoagland nutrition solution, and thereafter they were treated with pristine biochar and βS-MBC and Scandium solutions (Figure S2). The photoperiod and temperature were established at light/dark (13/11 h) and day/night 23/18°C, respectively, with RH (relative humidity) being 70 % and 850 μmol $m^{-2}.s^{-1}$ of PFD. Table 1 delineates methods of treatment employed in this research. Wheat seedlings were harvested 30 days post-sowing, purified with ultra-pure-water, desiccated, and preserved for later testing.

2.4. Assessment of roots characteristics and the biomass

Roots and shoots of plants were assessed for the root's characteristics, including weights (dry and fresh); via rinsing their tissues with DI water. Dry weight of roots and shoots was subsequently ascertained via dried plant specimens for 36 h. To examine morphological traits, 6 identical wheat plants were chosen from every treatment group. The WinRHIZO 2020a software (V. 5.51.0, China) was employed for root measurement and scanning, while Imagery X-ray Screen (was used to image the roots.

2.5. Oxidative stress markers, photosynthesis and activities of glyoxalase and antioxidant enzyme assessment

Konica Minolta SPAD-502Plus chlorophyll Meter was utilized to measure the relative chlorophyll content in completely developed wheat leaf. The methodology of Ghosh et al. (2022) was employed to quantify chlorophyll a and b as well as carotenoids, with absorbance measured using a spectrophotometer at 663 and 646 nm (Eqs. 1, 2 and 3). Gas exchange characteristics, including transpiration rate (Tr), photosynthetic rate (Pn), stomatal conductance (Gs) following the protocol by Qin et al. (2024), and intercellular carbon dioxide concentration (Ci), were evaluated utilizing a portable infrared gas analyzer (IRGA). These parameters were assessed between 10.30 a.m. and 1 p.m. when the plants were fully functional.

$$Chla \quad \left(\frac{mg}{g}\right) = [12.7(A663) - 2.69 \quad (A645) \times V \Big/ W \tag{1}$$

$$Chlb \quad \left(\frac{mg}{g}\right) = [22.9(A645) - 4.68 \quad (A668)] \times V \Big/ W \tag{2}$$

$$Carotenoids\left(\frac{mg}{g}\right) = [(1000 \times A470) - (3.27 \times Chla + 104 \times Chlb)] \times V \Big/ W \tag{3}$$

Table 1
Treatments plan used in this experiment.

Treatments	Details	Dose levels
Control	Without pristine biochar, βS-MBC and Scandium	-
PBC	Pristine biochar	3 %
βS-MBC	β-sulfur modified biochar	3 %
Sc40	Only Scandium	40 mg L^{-1}
Sc40 +PBC	Pristine biochar + Scandium	40 mg L^{-1} + 3 %
Sc40 + βS-MBC	β-sulfur modified biochar + Scandium	40 mg L^{-1} + 3 %

To ascertain the concentrations of soluble protein, ascorbate (AsA) and glutathione (GSH), 0.2 g specimen from shoots and roots was treated with phosphate buffer solution (10 % and 0.1 M) and subsequently centrifuged at 2500 g for 15 min. The supernatant was subsequently utilized to quantify soluble protein, AsA and GSH with kits G0212F (Suzhou Keming Biological Co., Ltd, China). The absorbance values of soluble protein, AsA and GSH were measured at 595, 540 and 600 nm, respectively.

6 identical plant roots and leaves analyzed to assess EL using methodology established by Angmo et al. (2023). The concentrations of malondialdehyde (MDA), superoxide anion (O_2^-) and hydrogen peroxide (H_2O_2) and proline quantity in root and leaf was assessed with supernatant obtained following total protein exploration. Hydrogen peroxide (H_2O_2), superoxide anion (O_2^-), malondialdehyde (MDA) and proline levels were measured utilizing the methodologies specified in A0145, A0652, A01569 and A01789 kits (Suzhou Keming Biological Co., Ltd, China). The methylglyoxal (MG) concentrations in leaves and roots were evaluated with the methodology described by Yang et al. (2021).

The supernatant obtained after the total soluble protein determination was utilized to assess enzymatic activity. The enzymatic activities of monodehydroascorbate reductase (MDHAR), dehydroascorbate reductase (DHAR), glutathione reductase (GR), ascorbate peroxidase (APX), catalase (CAT) and superoxide dismutase (SOD) were evaluated in leaves and roots utilizing a methodology established for BC0650, BC0660, A123–1–1, A062–1–1, A007–1–1 and A001–4 kits (Suzhou Keming Biological Co., Ltd, China). The activities of glutathione-dependent enzyme in wheat roots and leaves were assessed. The activities of GPX and GST were evaluated based on instructions included in A-254 and A-2541 kits (Suzhou Keming Biological Co., Ltd, China). The methodology established by Laus et al. (2023) was employed to assess Gly-I and Gly-II enzymatic activities, utilizing extinction values of 13.6 and 3.37 mM^{-1} cm^{-1}.

2.6. Quantification of Sc

The Sc concentrations in wheat roots and leaves were measured using graphite furnace-based AAS (Atomic absorption spectroscopy) (AA320N, AELAB, China), as outlined by Shtangeeva (2022).

2.7. Analysis of gene expression

Total RNA obtained from roots and leaves specimens was determined utilizing the Trizol technique according to manufacturer's procedure. A Nano-drop UL2000 spectrophotometer utilized to evaluate total RNA level, while agarose-gel electro-phoresis conducted to confirm total RNA quality and purity. cDNA was synthesized from extracted RNA through reverse transcription polymerase chain reaction (RT-PCR) using a Vazyme HiScript-II QRT SuperMix Kit. qRT-PCR was conducted on 96-well plates using a qTOWER3 QPCR apparatus and FastStart Essential DNA Green Master Kit according to the manufacturer's instructions. OsUbiquitin was applied as reference gene under stress from metals (Soni et al., 2021). The $2^{-\Delta\Delta CT}$ formula was utilized to ascertain the relative level of gene expression (Wu et al., 2024). Table 2 enumerates primers employed in this study.

2.8. Statistical analyses

The acquired data were subjected to statistical analysis utilizing SPSS (version 29). The data significance was evaluated by conducting Duncan's post hoc and one-way ANOVA tests, with $P < 0.05$ significance level. The data provided in graphs are represented as mean ± SE (standard error) of 6 replications. All charts were produced utilizing Excel and Origin programs.

3. Results

3.1. Biochar characterization

The biochar produced from rice husk wastes at lower temperatures exhibits a relatively high oxygen level, increased organic C, and a greater abundance of polar groups on the surface compared to the biochar generated at higher temperatures. The functional groups on biochar surface may diminish as carbonization temperature increases. Thus, 500 °C was designated as temperature of pyrolysis for this study. Table 3 indicates that relative to pristine biochar, β-S treatment exhibited enhancements in SSA (61.22 %), ash level (19.39 %), carbon level (9.02 %), and 3-units increase in pH in βS-MBC (8.91) relative to pristine biochar. Numerous studies have documented favourable alterations in surface characteristics of treated pristine biochar. The βS-MBC exhibited elevated O/C as well as H/C molar ratio, recorded at 0.101 and 0.047, compared to pristine biochar.

3.2. Pristine biochar and βS-MBC attributes

The adsorption of pollutants on biochar is directly contingent upon its surface characteristics. The analysis employed TEM and SEM approaches to examine surface and microstructures properties of pristine biochar and βS-MBC (Fig. 2a-d). The treatment of pristine biochar improved the surface structure, resulting in βS-MBC displaying finely

Table 3
Basic characteristics of pristine biochar and βS-MBC.

Properties	Pristine biochar	βS-MBC
Yield (wt%)	25.401 ± 2.119	34.803 ± 2.3
Ash level (wt%)	20.239 ± 2.350	16.180 ± 0.489
C (%)	70.110 ± 1.982	63.200 ± 3.100
H (%)	1.241 ± 0.188	1.800 ± 0.089
O (%)	8.112 ± 0.359	11.301 ± 0.389
N (%)	1.480 ± 0.049	0.760 ± 0.040
C+H+O+N	76.202 ± 4.125	77.51 ± 4.300
H/C	0.050 ± 0.002	0.039 ± 0.002
O/C	0.119 ± 0.003	0.160 ± 0.006
(N + O)/C	0.129 ± 0.006	0.169 ± 0.020
pH	8.990 ± 0.502	6.102 ± 0.402
EC (Cmol kg^{-1})	95.302 ± 4.449	250.130 ± 15.50
SSA (m^2 g^{-1})	30.112 ± 2.115	100.120 ± 5.021

EC = Effective Cation Exchange Capacity (ECEC); SSA = specific surface area

Table 2
Sequences of gene-specific primers utilized in the current research.

Objectives	Gene Name	Accession No.	Forward (5'-3')	Reverse (5'-3')
Reference gene	*OsUBQ*	L31941	GACGGACGCACCCTGGCTGACTAC	TGCTGCCAATTACCATATACCACGAC
Target genes	*OsCuZnSOD1*	AK061662	ATGCGTCTGTGTTGCTTCTG	CCATCTCCCTCTTGGACAAA
	OsCaTB	KR133179	GTGAATGCACCAAAATGTGC	CCAGCCTGTTGGAAATTGTT
	OsGPX1	AY100689	TGAACCGGTCCCATATGAAT	AGCGGTGTAAGGTGAAATGG
	OsGSTU37	AF402799	GCTGAGTCTGCCGGATAGAG	ATTTATTCCCAGGTGGCACA
	OsAPX2	AB053297	TCAAGGACCAACTTCCCATC	AGGGTGTGACCACCAGAAAG
	OsGLYI-1	KC857628	AATTTTGTTCTTGGCGATGG	CTTATTGGGTGGCATGCTCT
	OsGLYII-2	AY054407	CTCGCCAAGAGACCATAAGC	GCTCTCGTCCACGATTCTTC
	OsFSD1	AK062073	AACAACGGCAACCCATTACCA	CCTGGTGACCCACCACCTTC

porous configuration (Fig. 1d). The predominant nanoparticles size ranged from 3 to 32 nm, signifying the existence of uncluttered β-S-functionalized layered structure (Fig. 1a-d).

FTIR spectroscopy was employed to ascertain functional groups existing on pristine biochar and βS-MBC surfaces (Fig. 2a). Spectra indicate that functional groups in pristine biochar and βS-MBC are notably similar, with discrete absorption bands distinguishing surface functional groups. FTIR peaks signify the existence of functional groups such as Fe-O, C-C-C, COOH/CHO, C═C and -O-H (Fig. 2a). XRD peaks for βS-MBC were more prominent and had greater intensities than those of pristine biochar as illustrated in Fig. 2b. This implies improved crystallinity or more structural order in βS-MBC, signifying that β-S treatment was more efficacious in augmenting pristine biochar structure. Pristine biochar elevated baseline intensity indicates greater occurrence of disordered components or amorphous C. The β-S additions seem to diminish the amorphous level, yielding more distinct and sharper peaks. Although no discernible alterations in the peak shoulder sites were seen between pristine biochar and βS-MBC, any minor displacement in peak positions may suggest that β-S was infiltrating the pristine biochar structure and altering the crystalline areas interplanar spacing. The insertion of β-S resulted in β-S-functionalized structures, as seen by alterations in the pattern of XRD (Fig. 2b). The βS-MBC diminished baseline intensity was due to a decreased amorphous carbon concentration.

EDS was employed to determine the elemental content of pristine biochar and βS-MBC. Elemental analysis of pristine biochar and βS-MBC demonstrated a consistent elemental distribution. The elements Ca, K, Mg, P, Si, S, Fe, O and C were seen to be evenly distributed on the surface of βS-MBC (Table 4). The proportions of primary components identified on pristine biochar/ βS-MBC surfaces are as follows: 0.89 % Ca, 0.03 % K, 0.10 % Mg, 0.16 % P, 1.03 % Si, 0.30 % S, 1.03 % Fe, 23.88 % O and 73.41 % C, respectively (Table 4). The concentrations of Ca, Mg, Si, S, and O in βS-MBC were elevated with β-S treatment in comparison to pristine biochar. The augmented presence of sulfur-containing groups on the βS-MBC surface, due to sulfur modification, improved the material's attraction for metallic ions.

3.3. Root morphology, wheat growth and Sc deposition in leaves and roots

The results indicated that the fresh weight and dry weight of wheat shoots in Sc-stressed plants were diminished; It was found that the fresh weight dropped by 44.11 % and the dry weight by 40.22 %, alongside root fresh weight and dry weight by 49.23 % and 65.30 %, respectively, in comparison to the controls (Fig. 3a-d). Nevertheless, utilization of pristine biochar and βS-MBC markedly enhanced shoot fresh weight by 29.88 % and 59.39 %, and dry weight by 27.74 % and 46.60 %, in addition to root fresh weight by 35.70 % and 59.11 %, and dry weight by 89.29 % and 119.71 % under Sc stress relative to the controls (Table 5). The utilization of pristine biochar and βS-MBC enhanced both root and shoot fresh and dry weight in wheat plants not exposed to Sc stress, in comparison to the control.

Regarding deposition in wheat leaves and roots, the Sc level was significantly elevated in Sc-stressed treatments (Fig. 3e). Pristine biochar addition diminished the Sc concentration by 35.09 % in leaves and by 26.01 % in roots of 'pristine biochar + Sc' plants relative to the Sc-treatment. βS-MBC treatment diminished Sc accumulation by 37.10 % in leaves and by 25.11 % in roots of the 'βS-MBC + Sc' plants relative to 'pristine biochar + Sc' plants. Both pristine biochar and βS-MBC addition facilitated wheat development under Sc stress; however, βS-MBC was more efficacious in diminishing Sc accumulation in both leaves and roots compared to pristine biochar.

Sc-stress adversely affected root characteristics (Figure S1). Sc stress reduced root length (47.69 %), surface area (59.59 %), root tips (49.79 %), root volume (48.20 %), root crossings (60.40 %) and root forks (40.41 %) in comparison to controls. Pristine biochar addition markedly enhanced root length (40.60 %), surface area (70.11 %), root volume (40.20 %), root tips (29.30 %), root crossings (46.71 %) and root forks (20.49 %), in comparison to Sc-stressed plants. The βS-MBC incorporation into Sc-treated plants led to enhancements in root length (20.11 %), surface area (25.80 %), root volume (24.61 %), root tips (15.30 %), root crossings (19.37 %) and root forks (14.18 %), relative to the 'pristine biochar + Sc' plants.

3.4. Photosynthesis traits

The results demonstrated that Sc-stress adversely affected SPAD

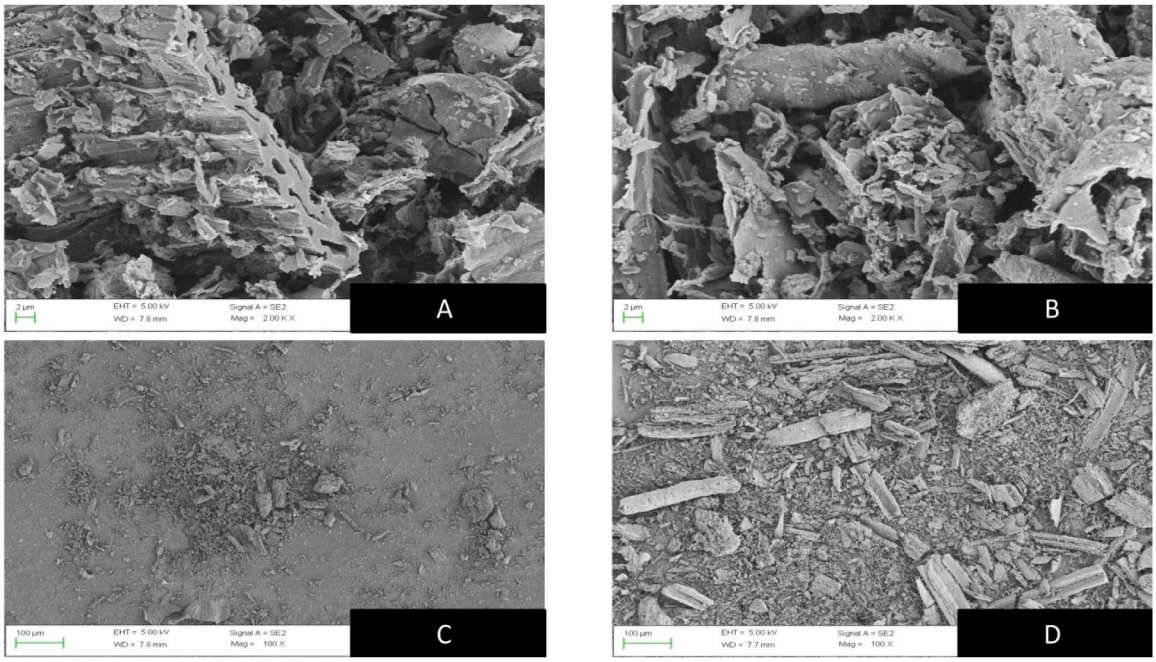

Fig. 1. SEM pictures of (a) pristine biochar, (b) βS-MBC. TEM images of (c) pristine biochar, (d) βS-MBC.

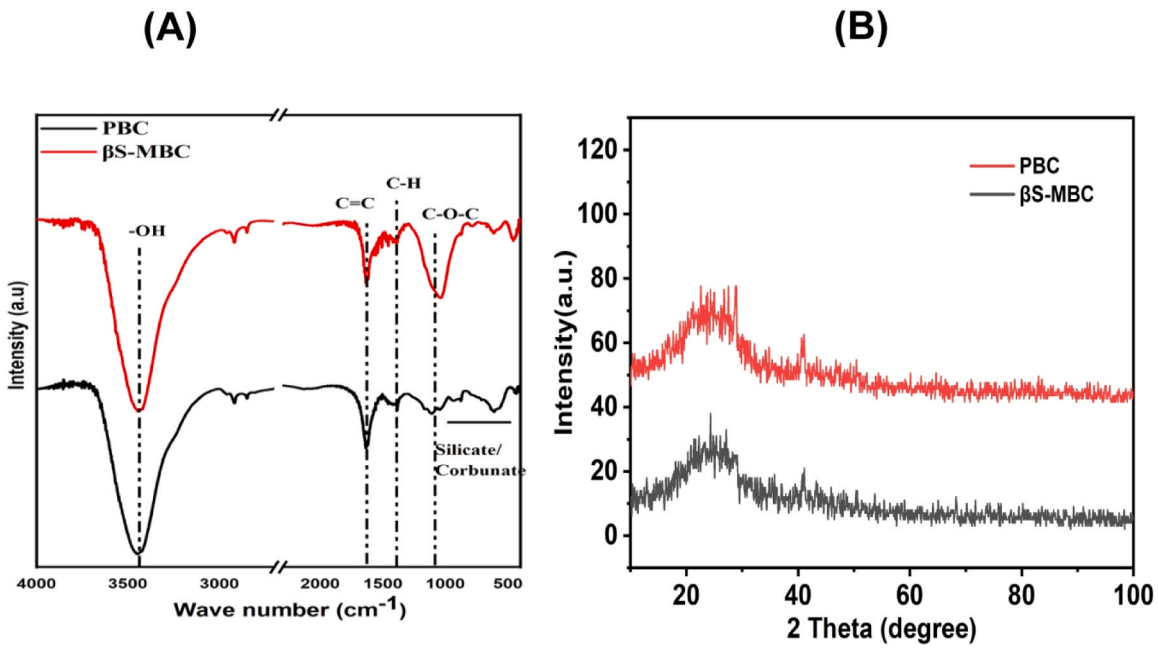

Fig. 2. (A) FTIR spectrum and (B) XRD analysis of pristine and β-Sulfur-engineered rice husk biochar.

Table 4
Elemental dispersion of Ca, K, Mg, P, Si, S, Fe, O and C in PBC and βS-MBC.

Elemental Properties (wt%)	Pristine biochar	βS-MBC
Carbon	74.40	66.69
Oxygen	23.97	28.11
Iron	1.02	0.55
Sulfur	0.27	0.60
Silicon	1.03	2.30
Phosphorus	0.16	0.16
Magnesium	0.12	0.24
Potassium	0.03	0.03
Calcium	0.88	2.39

index and chlorophyll levels in this research. Sc-stressed plants showed a reduction in SPAD index (50.11 %), carotenoids (51.19 %), Chl-a (49.30 %), Chl-b (48.31 %) relative to corresponding values in control plants (Table 5). The utilization of pristine biochar in Sc-treated plants facilitated maintenance of SPAD index (28.10 %), carotenoids (37.10 %), Chl-a (50.80 %), Chl-b (26.70 %), and in comparison, to Sc-stressed wheat. βS-MBC showed superior efficacy relative to PBC, enhancing SPAD index (20.11 %), carotenoids (11.99 %), Chl-a (10.29 %) and Chl- b (19.54 %) under Sc stress than 'PBC + Sc' treatment. Furthermore, Tr (55.98 %), Ci (39.20 %), Gs (58.10 %) and Pn (47.50 %) exhibited considerable reductions during Sc stress in comparison to control (Table 6). The application of PBC markedly enhanced Tr (39.20 %), Ci (24.10 %), Gs (49.30 %) and Pn (16.59 %) in 'PBC + Sc' plants relative to 'Sc' plants. The βS-MBC treatment significantly improved Tr (19.78 %), Ci (16.30 %), Gs (29.60 %) and Pn (20.40 %) in 'βS-MBC + Sc' plants relative to 'PBC + Sc' plants.

3.5. Oxidative stress

Sc contact in wheat generated reactive oxygen species (ROS), which adversely affected their growth. Our research indicated that Sc stress greatly elevated concentrations of EL (329.40 %/300.69 %), MDA (139.91 %/150.80 %) and H_2O_2 (130.59 %/179.20 %) in roots and leaves, in comparison to the control (Fig. 4, Table 5). PBC addition in Sc-stressed plants lowered H_2O_2 levels by 15.35 %/16.20 %, EL by 26.40 %/28.23 %, MDA by 20.81 %/25.90 % and $O_2^{\cdot}$ by 18.19 %/16.91 %, in roots/leaves, respectively, in comparison to 'Sc' plants. The 'βS-MBC treatment decreased H_2O_2 concentrations by 20.10 %/17.61 %, EL by 18.21 %/18.89 %, MDA by 18.59 %/13.80 % and $O_2^{\cdot}$ by 15.29 %/16.02 % in roots/leaves of 'βS-MBC + Sc' plants relative to 'PBC + Sc' plants. In comparison of PBC and βS-MBC treatments with the control, βS-MBC showed superior efficacy in mitigating ROS damage compared to PBC. Additionally, ASA and protein concentrations in roots and leaves diminished by 56.21 % and 54.22 %, and 53.29 % and 55.97 %, respectively, whereas GSH levels increased by 63.10 % and 64.30 % in roots and leaves under Sc stress compared to the control (Fig. 4). The PBC incorporation elevated protein level by ASA by 35.20 %/35.60 % and 34.49 %/34.70 %, while diminishing GSH by 13.60 %/11.32 % in the roots/leaves of 'PBC + Sc' plants relative to 'Sc' plants. The βS-MBC treatment elevated ASA by 21.10 %/23.11 % and protein level by 28.49 %/26.20 %, while diminishing GSH by 15.80 %/20.11 % in roots/leaves of 'βS-MBC + Sc' plants relative to 'PBC + Sc' plants.

3.6. Glyoxalase and antioxidant enzymes

Sc stress greatly diminished the glyoxalase and antioxidant enzyme activities (Table 7). The PBC and βS-MBC supplied mitigated Sc toxicity thru increasing glyoxalase and antioxidant enzyme activities while decreasing MG and ROS formation in wheat, in contrast to Sc-stressed crops (Fig. 5). βS-MBC treatment markedly enhanced antioxidant enzymatic activities, CAT (99.89 %/120.12 %), Gr (59.43 %/199.19 %), SOD (91.39 %/86.31 %), GST (120.81 %/131.69 %), GPX (81.91 %/84.19 %), MDHAR (91.11 %/86.38 %), DHAR (63.11 %/54.59 %) and APX (64.69 %/90.31 %) in roots and leaves of 'βS-MBC + Sc' plants in comparison to 'Sc' plants (Table 7, Table 5). Furthermore, PBC and βS-MBC treatments mitigated MG toxicity through enhancing the expression of Gly-I and II in reaction to Sc toxicity (Table 7). The βS-MBC treatment increased Gly-I by 80.09 %/100.20 % and Gly-II by 100.30 %/120.33 %, while decreasing MG concentrations by 33.01 %/34.10 % in roots and leaves than control.

3.7. Genes encoding antioxidants

To investigate genetic mechanisms underlying antioxidative defensive mechanisms activated by PBC and βS-MBC in plants, expression

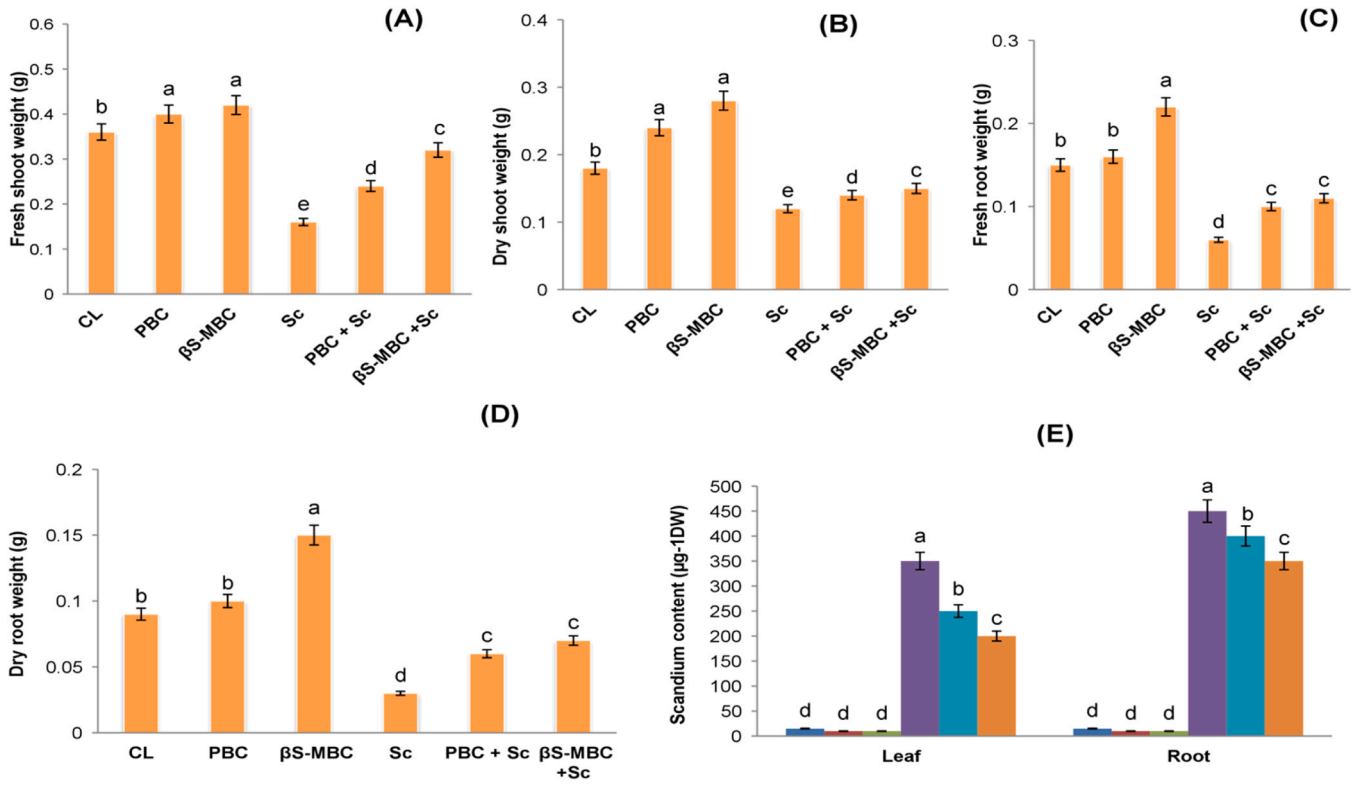

Fig. 3. Effects of pristine biochar (PBC) and β-sulfur-modified biochar (βS-MBC) on fresh shoot weight (a), dry shoot weight (b), fresh root weight (c), and dry root weight (d). Accumulation of Scandium in the roots and leaves under conditions of Scandium stress, the bars represent the mean ± standard error (n = 6). Distinct lowercase letters indicate significant differences among treatments ($P < 0.05$).

Table 5
Results of one-way ANOVA regarding the effect of βS-MBC on wheat growth metrics under Scandium (Sc) stress.

						Leaves		Roots	
Variable		**F**	**P**	**Variable**		**F**	**P**	**F**	**P**
Agronomy traits	FW shoot	59.08	0.00	Antioxidant enzymes	SOD	153.67	0.00	83.95	0.00
	DW shoot	659.81	0.00		CAT	96.03	0.00	38.32	0.00
	FW root	14.71	0.00		APX	754	0.00	289.8	0.00
	DW	161.9	0.00		GPX	150.55	0.00	337.55	0.00
Root traits	Root length	279.67	0.00		GR	105.38	0.00	283.75	0.00
	Root volume	149.79	0.00		GST	178.42	0.00	240.25	0.00
	Root fork	143.66	0.00		DHAR	167.35	0.00	330.15	0.00
	Root tip	1157.57	0.00		MDHAR	169.37	0.00	121.24	0.00
	Surface area	98.62	0.00		GLY-I	71.44	0.00	125.12	0.00
	Root crossing	322.9	0.00		GLY-II	244.81	0.00	191.35	0.00
Photosynthesis traits	Chl a	202.76	0.00		MG	62.43	0.00	89.78	0.00
	Chl b	132.33	0.00		H_2O_2	623.2	0.00	233.51	0.00
	Carotenoids	725.45	0.00		$O_2^{\bullet-}$	239.34	0.00	97.08	0.00
	SPAD index	218.74	0.00		MDA	245.13	0.00	176.22	0.00
	Pn	144.88	0.00		EL	513.74	0.00	556.15	0.00
	Tr	474.8	0.00		Protein	161.9	0.00	113.09	0.00
	Gs	138.3	0.00		Sc accumulation	73019	0.00	61526.8	0.00
	Ci	216.2	0.00						

profiles of 8 genes-*OsCaTB, OsCuZnSOD-1, OsGSTU37, OsGPX-1, OsGLY1–1, OsAPX-2, OsFSD-1* and *OsGLY11–2* measured (Figure 5Aa-h). The findings indicated that Sc stress decreased expression patterns of antioxidant-based genes, but βS-MBC markedly increased their expression, demonstrating statistical significance in comparison to control.

Expression degrees of *OsFSD1, OsGLY11–2, OsGLY1–1, OsAPX-2, OsGSTU37, OsGPX-1, OsCaTB* and *OsCuZnSOD-1* were elevated in roots and leaves of 'βS-MBC + Sc' by 60.19 %/57.30 %, 55.90 %/159.91 %, 58.81 %/60.11 %, 70.29 %/110.71 %, 99.10 %/160.28 %, 71.80 %/110.11 % and 100.59 %/110.49 %, respectively, in comparison to control (Fig. 5). The most elevated expression patterns of these genes were noted in 'βS-MBC + Sc' plants. The results indicate that βS-MBC significantly influenced gene expression during Sc stress ($P < 0.05$).

4. Discussion

This study reveals the effectiveness of β-Sulfur-engineered Biochar (βS-MBC) in alleviating Scandium toxicity in wheat, a significant issue in agricultural soils polluted with rare earth elements. Our results indicate that βS-MBC markedly enhanced wheat growth traits, photosynthetic efficiency, and redox control, highlighting its potential as an innovative soil amendment. Novel sulfur-engineered structure of βS-MBC facilitates improved adsorption of Sc, diminishing its bioavailability and toxicity, while fostering crop growth and physiological processes. This discourse

Table 6
Assessment of photosynthetic pigments in wheat plants subjected to Sc stress, following treatment with pristine and modified biochars.

Treatments	Chl a (μg g^{-1} FW)	Chl b (μg g^{-1} FW)	Carotenoids (μg g^{-1} FW)	SPAD index	Ci (μM CO_2 m^{-2} s^{-1})	Pn (μM m^{-2} s^{-1})	Gs (mM H_2O_2 m^{-2} s^{-1})	Tr (mM H_2O_2 m^{-2} s^{-1})
Control	1.28 ± 0.05 f	0.50 ±.0.04 g	0.59 ± 0.04 f	0.29 ± 0.05 f	13.01^{ab}	21^{b}	1.40^{b}	3.40^{b}
PBC	1.87 ± 0.05a	1.10 ± 0.03a	0.39 ± 0.06d	0.45 ± 0.03c	14.21^{a}	22^{a}	1.81^{a}	6.81^{a}
βS-MBC	2.11 ± 0.07a	1.23 ± 0.05a	0.66 ± 0.05a	0.65 ± 0.08a	15.03^{a}	25^{a}	2.17^{a}	8.17^{a}
Sc40	1.69 ± 0.09c	0.79 ± 0.07b	0.59 ± 0.06a	0.39 ± 0.04c	12.12^{b}	10^{d}	0.70^{d}	2.70^{d}
Sc40 +PBC	1.51 ± 0.06b	0.59 ± 0.06 f	0.47 ± 0.06b	0.45 ± 0.04c	12.1^{b}	17.10^{b}	1.20^{c}	4.20^{c}
Sc40 + βS-MBC	1.39 ± 0.11c	0.69 ± 0.04c	0.47 ± 0.08 f	0.30 ± 0.05 f	14.39^{b}	14.50^{c}	1.23^{c}	5.23^{c}

situates these results within extensive literature on biochar modifications, emphasizing distinctive benefits of βS-MBC in mitigating Sc toxicity and its ramifications for sustainable environmental remediation and agriculture.

4.1. Attributes of PBC and βS-MBC

Biochar engineering can improve its surface characteristics, potentially aiding in mitigation of heavy metal contamination. SEM scans of PBC and βS-MBC carbonized at 500 °C that they had a microporous structure, corroborating results of Huang and Imran (2025). The sulfur presence on the βS-MBC surface may have resulted in a higher quantity of irregularly shaped particles. Elemental analysis verified effective sulfur integration into βS-MBC surfaces, which is essential for its efficacy in heavy metal adsorption. The integration of sulfur into biochar surface enables effective heavy metal adsorption through mechanisms such as complexation and precipitation. Sulfur-containing functional groups, particularly thiol (-SH) and sulfide (S^{2-}) groups, exhibit a strong affinity for heavy metal ions, forming stable complexes and precipitates that reduce metal mobility and bioavailability. This specific interaction enhances the adsorption capacity of sulfur-modified biochars, making them efficient sorbents for heavy metal removal from contaminated environments (Jiang et al., 2025; Murtaza et al., 2024a). Zhao et al. (2020) identified a sulfur level of 0.7 % in sulfur-modified biochar. Our findings indicated following sulfur transformation, contents of O, N and C in biochar diminished, whilst the H level increased, leading to an elevation in the aromaticity degree and reduction in polarity. Consequently, both PBC and βS-MBC exhibited reduced hydrophilicity and an increased presence of aromatic structures, enhancing their capacity to interact with and sequester metallic ions (Peng et al., 2025).

The significant pH drops from pristine biochar (PBC, 8.99) to βS-modified biochar (βS-MBC, 6.10) critically influenced Sc bioavailability and wheat growth. The acidic βS-MBC (pH 6.10) increased Sc^{3+} solubility, enhancing its potential uptake by plants. However, sulfur functional groups (-SH, -S-S-) in βS-MBC effectively chelated Sc, immobilizing it and reducing toxicity, which promoted plant growth (+59.39 % shoot fresh weight and +49.30 % Chl-a). In contrast, alkaline PBC (pH 8.99) likely precipitated Sc as insoluble hydroxides/oxides, lowering bioavailability but without effective sequestration, possibly limiting nutrient availability and stressing plants. Thus, βS-MBC's acidic pH and sulfur groups synergistically enhanced Sc immobilization, overriding increased solubility, explaining its superior efficacy in mitigating Sc toxicity and boosting growth.

Biochar's adsorption capacity is significantly influenced by functional groups on the biochar surface. Biochar functional groups analyzed pre-and-post-modification via FTIR, revealing the following functional groups: aromatic C =H, C-O-C, C = O, COOH, and C = C. The key functional groups present in βS-MBC were identified at SO_3^{2-}, C–O–C, COOH/CHO, C = C, C = O, aliphatic-CH_2, and -O-H. The biochar modification with beta-sulfur introduces new functional groups, augmenting its adsorption capacity. The presence of SO_3^{2-} groups facilitates electrostatic interactions with positively charged contaminants, while C–O–C and COOH/CHO groups promote complexation and hydrogen bonding. The C═C and C═O functional groups facilitate π-π interactions and electron donor-acceptor interactions, respectively. The aliphatic -CH_2 and -O-H groups enhance hydrophobicity and reactivity. The functional groups collaborate to augment the adsorption capacity of beta-sulfur modified biochar for diverse contaminants via mechanisms including complexation, electrostatic interactions, hydrogen bonding, and π-π interactions (Murtaza et al., 2024b). These results indicate βS-MBC possesses a broader intricate functional group composition than other substances, which may enhance its adsorption and reactivity capacity for scandium and other heavy metals.

4.2. Root architecture and plant growth response to βS-MBC

The present research found that scandium stress greatly diminished crop growth and biomass. The mechanism underlying this decline is mostly attributed to scandium's capacity to impair chloroplasts, resulting in diminished levels of photosynthetic pigments, which consequently decreases photosynthesis. Scandium stress significantly diminishes crop growth by altering metabolic pathways and hindering cell division (Junior et al., 2021). Conversely, application of βS-MBC significantly improved growth and biomass output in scandium-contaminated wheat plants, presumably because of increased nutrient accessibility from βS-MBC. This aligns with analogous beneficial impacts of modified biochar on various crops (Kumar et al., 2025; Murtaza et al., 2025b). The enhancements in growth are attributed to the improved CEC (cation exchange capacity) and elevated nutritional status resulting from biochar incorporation (Pan et al., 2025). Furthermore, Singh et al. (2025) showed that crop growth characteristics were enhanced due to biochar treatment, consistent with our findings. Furthermore, our research revealed that scandium toxicity diminishes root growth, leading to a decrease in root volume, root tips, root fork numbers and surface area, which is ascribed to nutritional imbalances and reactive oxygen species formation, culminating in oxidative harm to the root cells. Cellular damage might hinder a plant's ability to absorb nutrients and water, thereby diminishing growth. Kumar et al. (2022b) similarly showed that decreased mitotic proliferation in chickpea under metal stress led to a decrease in root development. Our findings indicated that βS-MBC treatment markedly improved root characteristics under scandium stress by reducing root scandium uptake and augmenting antioxidant enzymatic activities that mitigate ROS-caused scandium oxidative stress, hence safeguarding root cells. The sulfur modification procedure incorporates functional groups (-C-S-C-, -C═S) that interact with Sc, diminishing its toxicity and bioavailability. This allows βS-MBC to mitigate Sc-induced stress, hence enhancing root growth and development, as seen by the enhanced root features noted in our research.

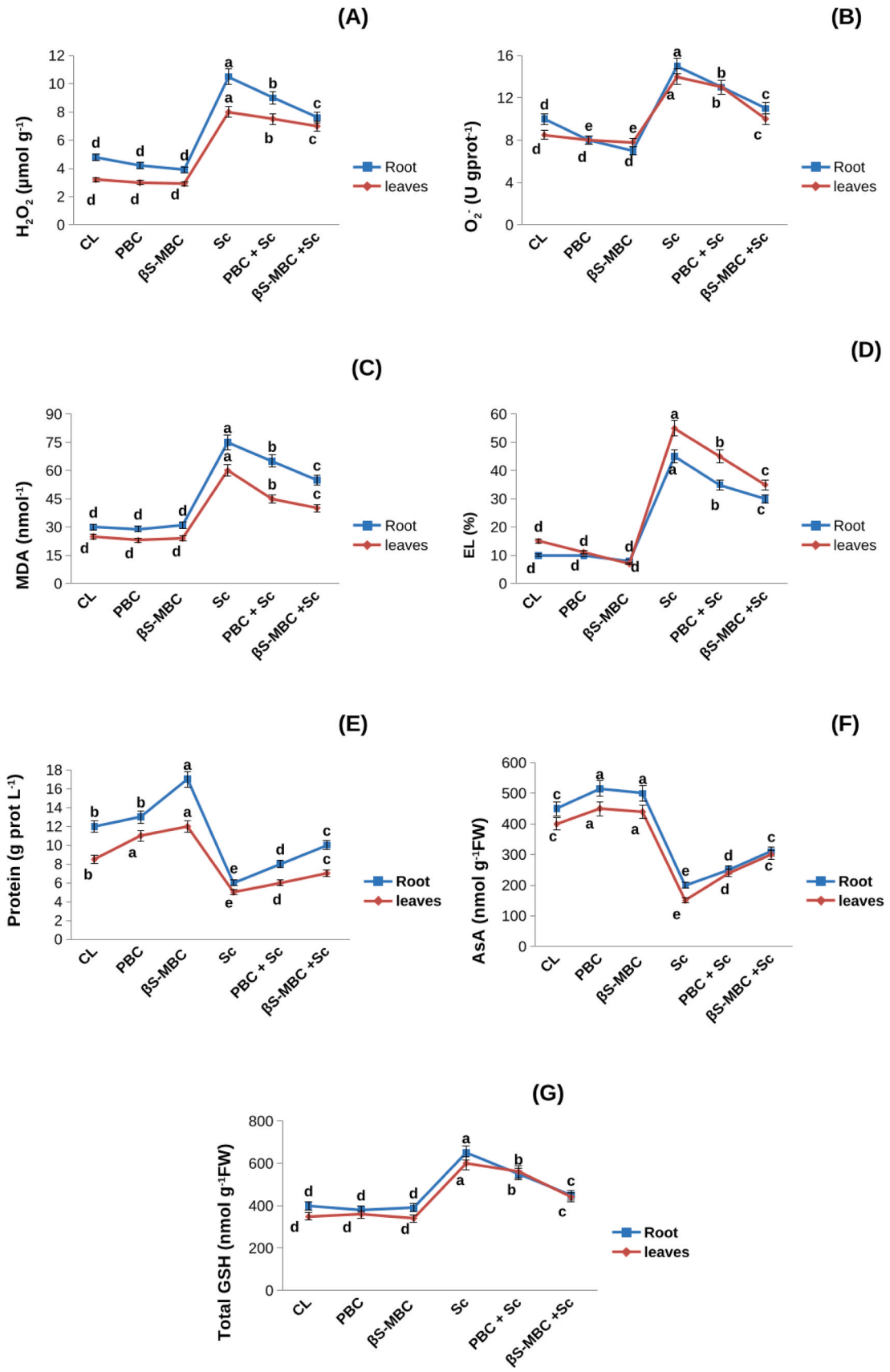

Fig. 4. Impact of PBC and βS-MBC treatment on (A) H_2O_2 (B) O_2^- (C) MDA (D) EL (E) Protein (F) AsA (G) Total GSH in roots and leaves subjected to Sc stress. The bars reflect the standard error of means (n = 6). Distinct lower-case letters denote statistically significant differences among treatments at $P < 0.05$.

Table 7
Impact of PBC and βS-MBC treatment SOD (U g^{-1} FW), CAT (U mg^{-1} protein), GPX (nM min^{-1} mg^{-1} protein), GST (U mg^{-1} protein), APX (U mg^{-1} protein), GR (U mg^{-1} protein), DHAR (U mg^{-1} protein), MDHAR (U mg^{-1} protein), MG (μmol g^{-1} protein), GLY-I (nmol min^{-1} mg^{-1} protein) and GLY-II (nmol min^{-1} mg^{-1} protein) levels in roots and leaves under Sc stress conditions. The standard error of the means (n = 6) is indicated by the bars $P < 0.05$.

Treatments	SOD	CAT	GPX	GST	APX	GR	DHAR	MDHAR	MG	GLY-I	GLY-I
Control	20.10 ± 0.20b	26.11 ± 1.59e	30.02 ± 1.41e	41.32 ± 1.39e	43.11 ± 1.39e	0.23 ± 0.01e	40.11 ± 1.41e	44.13 ± 1.39e	23.11 ± 1.39e	29.11 ± 1.69e	27.13 ± 1.87e
PBC	22.18 ± 0.39c	55.52 ± 2.14ab	67.59 ± 2.7ab	77.60 ± 1.9ab	69.71 ± 2.3ab	0.41 ± 0.02ab	80.11 ± 1.3ab	71.70 ± 2.3ab	36.63 ± 2.6ab	56.52 ± 2.29ab	78.59 ± 3.3ab
βS-MBC	23.01 ± 0.41a	61.45 ± 1.69a	73.78 ± 1.87a	89.10 ± 1.91a	78.12 ± 1.91a	1.3 ± 0.04a	98.12 ± 1.01a	81.11 ± 1.91a	46.80 ± 1.91a	60.45 ± 1.78a	97.78 ± 1.99a
Sc	15.20 ± 0.30c	16.24 ± 0.47d	20.29 ± 0.51d	29.30 ± 0.49d	27.33 ± 0.49d	0.21 ± 0.02d	33.10 ± 0.50d	33.38 ± 0.49d	19.28 ± 0.51d	17.24 ± 0.50d	35.29 ± 0.78d
PBC +Sc	16.45 ± 0.22c	30.14 ± 0.61c	40.31 ± 0.30c	43.12 ± 0.29c	51.29 ± 0.29c	0.26 ± 0.01c	51.08 ± 0.10c	43.25 ± 0.29c	29.01 ± 0.26c	29.14 ± 0.60c	54.31 ± 0.28c
βS-MBC + Sc	16.89 ± 0.26bc	37.25 ± 0.64bc	43.30 ± 0.63bc	51.11 ± 0.59bc	59.11 ± 0.97bc	0.33 ± 0.03bc	57.08 ± 0.60c	47.10 ± 0.97bc	37.29 ± 1.7bc	38.25 ± 0.29bc	61.29 ± 0.87bc

4.3. PBC and βS-MBC enhanced photosynthesis under scandium stress

Plant development relies on photosynthesis, which becomes less efficient under metal stress (Zaman et al., 2025). We observed that scandium greatly reduced the SPAD index and chlorophyll pigments of wheat seedlings. The generation of reactive oxygen species may contribute to these decreases as ROS can impair chloroplast membrane and chlorophyll proteins, leading to a decline in the photosynthetic apparatus. A decline in chlorophyll input has been proven to decrease chlorophyll concentration in various crops, including tomato, mustard, watermelon and rice, in response to scandium stress (Elbasan et al., 2020). Consequently, the enhancement in photosynthetic characteristics attributed to βS-MBC is probably related to addition of sulfur. This improvement in chloroplast structure and function stabilizes membranes, bolsters antioxidant defensive mechanisms and enhances metabolic activities that produce NADPH and ATP, thereby increasing photosynthetic performance (Murtaza et al., 2025a). Moreover, elevated chlorophyll content may be stimulated by the augmented surface area with biochar modification, corroborated by a significant rise in chlorophylls and carotenoids associated with biochar exhibiting greater surface area (Zhu et al., 2025).

Metal stress adversely impacts plants' capacity to assimilate carbon dioxide and many metabolic processes (Sana, Aqeel et al., 2025). Nevertheless, βS-MBC fostered an environment conducive to enhancing these mechanisms in wheat. Previous studies corroborate our findings that scandium stress diminished photosynthetic characteristics (Kaur et al., 2024), primarily through chloroplast degradation. The βS-MBC improved leaf gas-exchange characteristics and chlorophyll pigments in wheat cultivated under scandium stress conditions. The impact of tailored biochar on the photosynthesis rate under stressful conditions has been thoroughly documented in various previous studies (Murmu et al., 2025). Moreover, the photosynthetic process was observed positively correlated with sulfur concentration, as confirmed thru enhanced photosynthesis following biochar addition in legumes (Yan et al., 2024).

4.4. Impact of PBC and βS-MBC on scandium accumulation in wheat plants

The decrease in scandium accumulation in wheat may result from scandium binding with substances in biochar. Although the precise mechanism is yet to be clarified, we hypothesize that the βS-MBC extensive surface area facilitates scandium ions adsorption in wheat roots or generates insoluble scandium-sulfur compounds, hence restricting scandium bioavailability. Zheng et al. (2024) found that copper ions adsorption on sulfur microparticles happens via moderate complexation, leading to Cu-S complexes formation, and sulfides generally have a very low solubility. Our data indicated that scandium preferentially accumulated in wheat roots, with diminished amounts in leaves. Scandium complexation with polar substances in wheat root cell walls may explicate elevated content of scandium in wheat root relative to shoot (Xiao et al., 2024). Comparable findings were documented in watermelon, mustard and rice (Wiche et al., 2023). The protein levels in wheat shoots and roots decreased during scandium stress, probably owing to overproduction of ROS, which caused protein's oxidation and degradation, ultimately leading to reduced protein levels. Elbasan et al. (2020) also noted this pattern in chickpeas, which corresponds with analogous results in various plants (Liu et al., 2020). Nonetheless, application of βS-MBC to scandium-affected wheat seedlings increased protein level, which appeared correlated with elevated enzyme activity. Furthermore, utilization of biochar facilitated optimal protein synthesis, as indicated by Hafeez et al. (2024).

The sulfur groups in βS-MBC facilitate scandium immobilization via adsorption and complexation processes. The -C-S-C-, -C═S generated during the modification process exhibit a strong attraction for Sc, resulting in stable complexes that diminish their bioavailability and mobility. This phenomenon is ascribed to soft Lewis's base characteristics of sulfur, which readily establishes covalent connections with scandium, a hard Lewis acid, thus immobilizing it. Moreover, sulfur groups may engage in redox processes, hence enhancing Sc immobilization. This method allows βS-MBC to efficiently alleviate Sc toxicity, hence enhancing the growth and development of plants. At molecular level, sulfur functional groups generated during modification operate as soft Lewis bases, transferring electrons to establish stable complexes with Sc^{3+} ions (a hard Lewis acid). This results in the creation of inner-sphere complexes, diminishing Sc bioavailability and mobility. Furthermore, sulfur groups may engage in redox processes, hence enhancing Sc immobilization. The Hard-Soft Acid-Base theory underpins this mechanism, wherein soft bases such as sulfur preferentially associate with hard acids like Sc^{3+}, facilitating efficient immobilization. This molecular interaction underpins βS-MBC's capacity to alleviate Sc toxicity and enhance plant development.

4.5. Antioxidant system response to βS-MBC treatment under scandium stress

Our investigation revealed that scandium stress markedly impeded wheat growth, diminished photosynthetic performance, and decreased the activities of CAT and SOD. These data align with literature indicating that contact with heavy metals impairs antioxidant system, which is crucial for sustaining cellular equilibrium and serve as a vital defence versus oxidative stress, hence exacerbating it (Abdelslam and El-khawaga, 2025).

The current research indicated that scandium stress induced ROS excessive formation, particularly MDA and H_2O_2 in wheat. Oxidative stress impaired oxidative responses of wheat seedlings and degraded cellular membrane integrity, demonstrating scandium stress significantly harms wheat seedlings. The elevation in MDA (150.90 %/150.81 %) and H_2O_2 (130.59 %/179.20 %) levels in roots and leaves

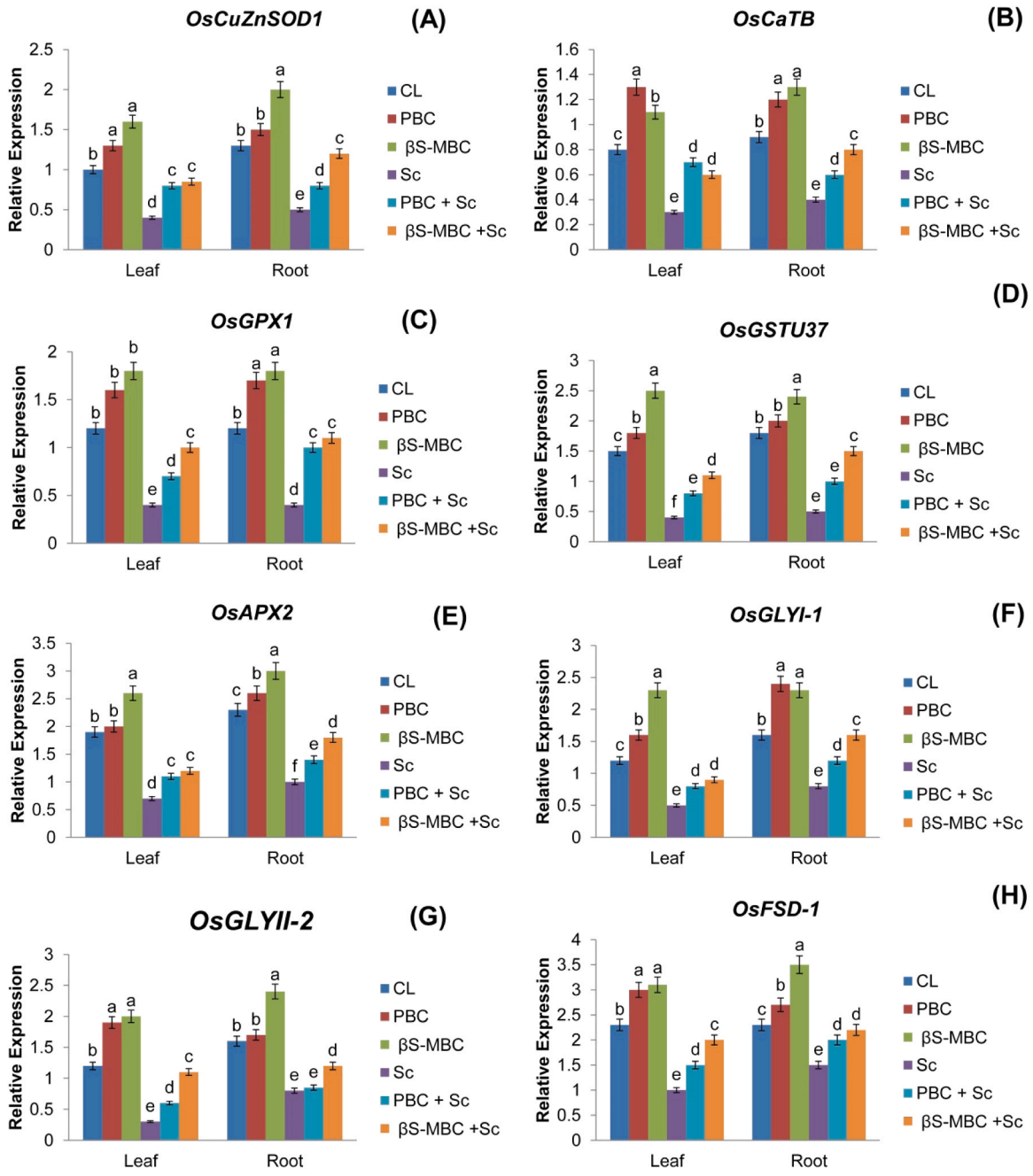

Fig. 5. Impact of PBC and βS-MBC treatment on relative gene expression related to glyoxalase and antioxidant defense systems in roots and leaves (A) *OsCuZnSOD1* (B) *OsCaTB* (C) *OsGPX1* (D) *OsGSTU37* (E) *OsAPX2* (F) *OsGLYI-1* (G) *OsGLYI-2* (H) *OsFSD-1* under Sc stress conditions. The bars reflect SE of means (n = 6). Distinct lower-case letters indicate substantial variances among applications at $P < 0.05$.

resulted from a disturbance in dynamic balance between reactive oxygen species and antioxidant enzymes. The PBC administration to scandium-stressed seedlings reduced concentrations of MDA and H_2O_2 as result of enhanced enzymatic activity. The results corroborated by evidence that βS-MBC diminished oxidative stress by augmenting antioxidant enzymatic activity (Wang et al., 2025; Lin et al., 2024). We additionally discovered that electrolyte leakage was markedly increased under scandium stress, presumably owing to reactive oxygen species (Wang et al., 2023). Our findings align with those reported by Kastori et al. (2023) noted elevated EL concentrations in reaction to scandium stress. The PBC administration to scandium-stressed seedlings led to decreased electrolyte leakage, likely associated with diminished ROS concentrations and membrane integrity preservation under metal stress conditions (Kanbar et al., 2021).

The current work reveals that scandium stress results in decrease in gene expression and antioxidant enzymes in wheat leaves and roots, while βS-MBC supplementation increases enzymatic activities. CAT elevation may mitigate ROS-caused oxidative harm by turning hydrogen peroxide into oxygen and water. The enhanced capacity of peroxidase to catalyze conversion of H_2O_2 into water reduces ROS harm to wheat. The increased activities of antioxidant enzymes jointly mitigate ROS-caused damage, sustain equilibrium between ROS generation and antioxidant enzymes, and ultimately promote crop growth. βS-MBC nourishing to wheat plants augmented Gly-I and II activities while diminishing MG concentration in wheat leaves in roots. Gly-I and II enzyme activity augmented to mitigate MG-caused toxicity in wheat and enhance scandium toxicity resistance. Increased enzymatic activity under scandium stress noted in various crops (Murtaza et al., 2025c). In contrast, βS-MBC

swiftly enhanced expression of genes *OsFSD1, OsGLYII-2, OsGR-2, OsAPX-2, OsGSTU37, OsGPX-1, OsCaTB* and *OsCuZnSOD-1* in response to scandium stress. Consistent with our findings, Ren et al. (2021) determined that addition of biochar enhanced enzyme activity under cadmium stress conditions. The purple mustard genotype demonstrates amplified gene expression associated with stress (Haider et al., 2025). The findings indicated that βS-MBC treatment demonstrated significant potential in mitigating scandium toxicity. The reduction of scandium bioavailability with the βS-MBC application diminished the scandium level in wheat tissues and lowered oxidative stress levels. The glyoxalase and antioxidant enzymes, which are responsible for reactive oxygen species and methylglyoxal detoxification, were elevated, resulting in diminished cellular damage. These findings indicate that βS-MBC may augment intrinsic defensive capabilities of wheat against detrimental effects generated by scandium, hence offering viable control strategy for heavy metal stress in cropping systems.

In this study, βS-MBC significantly diminished scandium levels in wheat tissue (Fig. 6). The findings indicate that βS-MBC may augment scandium bioavailability via many pathways, necessitating further investigation into processes such as chemical interactions, adsorption capacity, and physical effects, as outlined in the current literature. Adsorption is primarily acknowledged as the major mechanism by which biochar alleviates heavy metal stress. Current research indicates that biochar's higher porosity and surface area significantly enhance its ability for metallic ion adsorption. This work did not directly assess the βS-MBC adsorption ability; nevertheless, EDS analysis suggests that these traits may be augmented by sulfur addition. Existing evidence indicates that sulfur-rich functionalities can combine with heavy metals, potentially reducing their bioavailability. Furthermore, chemical interactions must not be disregarded in the discourse regarding the mitigation of scandium toxicity by βS-MBC. The sulfide disintegrates may be generated by sulfur, which likely stabilizes scandium ions, so restricting their accessibility for plant absorption. Sulfites or sulfate may specifically interact with scandium species to produce insoluble elements that mitigate adverse impacts of scandium on crops. This method underscores the critical importance of sulfur, even in minimal amounts, in alleviating scandium stress in wheat. The utilization of β-sulfur-engineered biochar (βS-BC) for Sc remediation has numerous beneficial side effects with little ecological or health hazards, as substantiated by evidence: βS-BC augments soil microbial diversity and activity, fostering beneficial bacteria such as *Bacillus* and *Pseudomonas* that facilitate nutrient cycling and plant growth (Deng et al., 2025). Its permeable structure enhances soil aeration, water retention, and cation exchange capability, hence augmenting plant resilience without leaching detrimental byproducts. Sulfur functional groups securely bind scandium, diminishing bioavailability and trophic transfer hazards, as demonstrated by reduced scandium levels in wheat shoots (this study) and decreased leachability in soil columns (Tomczuk et al., 2025). βS-BC further sequesters co-contaminants by S-metal chelation, enhancing soil remediation. Human health hazards are reduced since βS-BC undergoes pyrolysis (over 500 °C) to eradicate pathogens and poisons, while sulfur doping prevents the release of hazardous sulfur emissions (Deng et al., 2025). In summary, βS-BC adheres to One Health principles, promoting sustainable agro-ecological restoration.

4.6. *Detailed comparison of βS-MBC with other biochar modifications*

In contrast to traditional biochar modification techniques, β-sulfur-engineered biochar (βS-MBC) employed in this research has a distinct mechanism function that improves its ability to immobilize Sc^{3+} and mitigate potential phytotoxicity. Alkali/acid activation predominantly enhances porosity and surface area, while metal-oxide modification improves sorption via cation exchange and surface precipitation. Sulfur modifications, on the other hand, introduce strongly reactive functional compounds with a great affinity for metal binding. Significantly, β-sulfur produces a hybrid sulfur framework characterized by polysulfide connections and β-S chains, as opposed to the surface sulfates generated in alternative sulfurization methods. These β-S moieties have improved redox-buffering and electron-donating properties and establish more robust inner-sphere complexes with Sc^{3+}. Thus, βS-MBC reveals enhanced efficacy in decreasing bioavailable scandium, alleviating oxidative stress, and enhancing photosynthetic efficiency relative to other engineered biochars. The improved redox activity and prolonged metal binding afforded via β-S structures signify a notable progression beyond current modification methods and highlight the originality of this strategy. Comparison Table 8 given below

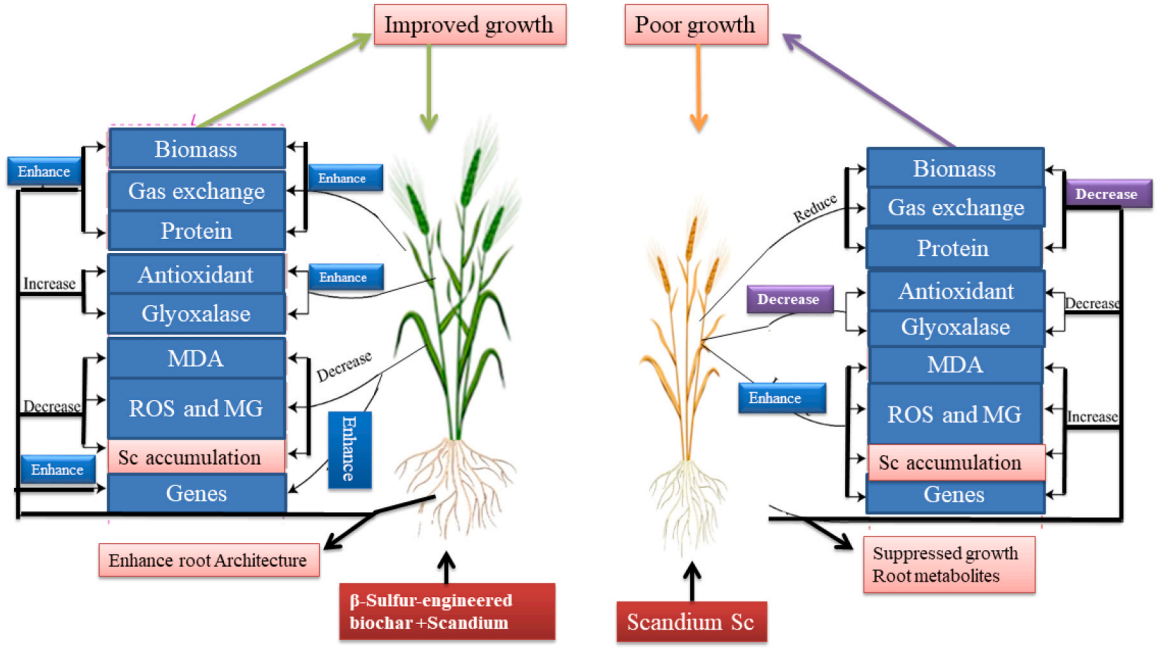

Fig. 6. Systematic depiction of the present research.

Table 8
comparison table with other modification and current study.

Modification type	Reference	Key Chemical Characteristics	Metal binding mechanism	Limitations	Significance to Scandium Treatment	Relative Novelty in Relation to βS-MBC
Alkali/acid Activation	Huang et al., (2022)	Enhanced porosity; -OH and -COOH functional groups formation	Surface complexation; enhanced adsorption resulting from increased SA	Restricted selection for trivalent metals; low redox capacity	Binds Sc weakly through oxygenated groups	βS-MBC provides enhanced Sc binding via sulfur donors and redox reactions
Metal-Oxide modification	Qu et al., (2023)	Metal oxides and hydroxides deposition	Cation exchange and surface precipitation	May disintegrate at fluctuating pH; competitive interaction with other cations	Elevated for certain metals, contingent upon the type of oxide; moderate for Sc	βS-MBC has greater stability and generates more robust inner-sphere complexes
Thiol-modification	Lyu et al., (2020)	Reactive thiol groups introduction	Robust affinity for malleable heavy metals	Thiols undergo oxidation readily; they less efficient for strong acids such as Sc	Thiols exhibit a preferential affinity for soft metals, excluding Sc	βS-MBC possesses polysulfide structures that more compatible with Sc
Sulfide modification	Lu et al., (2023)	Forms sulfide and sulfate groups on the surface	Ion exchange and precipitation of metal sulfates	Typically unstable; sulfur species susceptible to transition	Variable: restricted ability for stable Sc immobilization	βS-MBC offers more stable β-S chain configurations with enhanced affinity
β-Sulfur-Engineered Biochar (βS-MBC) (This study)	Current study	Prevalence of β-S chains and polysulfide connections; elevated redox activity	Robust inner-sphere complexation with Sc; improved electron transport and buffering capacity	Demands regulated synthesis; innovative way	Superior Sc immobilization, redox stabilization, enhanced plant performance	

5. Conclusion

This research shows that physicochemical traits of βS-MBC, compared to PBC, significantly enhance stress alleviation and plant nutrition. The findings indicated that βS-MBC significantly enhanced wheat growth under scandium stress by expediting seedling development and substantially reducing scandium accumulation in wheat tissues. Furthermore, the application of βS-MBC significantly affected essential physiological traits of crop, including leaf gas-exchange traits and chlorophyll contents. βS-MBC treatment promoted wheat growth more efficiently than PBC. The findings indicated that βS-MBC had positive impacts by enhancing antioxidant enzymatic activities, reducing ROS concentrations and diminishing gene expression associated with scandium stress resistance. The results underscore the viability of βS-MBC as a remedy for wheat adaptation to scandium stress. This work provides fundamental data for comprehending mitigation in wheat in reaction to scandium stress by βS-MBC. Future studies should systematically conduct adsorption tests to examine the βS-MBC adsorption ability for scandium and evaluate the postulated interaction processes among sulfur, scandium and PBC. Field experiments will be crucial to assess long-time advantages of βS-MBC in actual agricultural condition and to evaluate its viability as an ecologically sound way to alleviate heavy metal stress in plants.

Author's contribution

All authors contributed equally to the conception, designing, writing, reviewing, and approval of the final version of the manuscript.

CRediT authorship contribution statement

Rashid Iqbal: Writing – review & editing, Validation, Formal analysis, Data curation, Conceptualization. **Javed Iqbal:** Writing – review & editing, Validation, Formal analysis, Data curation, Conceptualization. **Sajid Ullah:** Writing – review & editing, Software, Formal analysis, Data curation, Conceptualization. **Khairiah Mubarak Alwutayd:** Writing – review & editing, Resources, Formal analysis, Data curation, Conceptualization. **Zeeshan Ahmed:** Writing – review & editing, Validation, Formal analysis, Data curation, Conceptualization. **Sajjad Hyder:** Writing – review & editing, Validation, Data curation, Conceptualization. **Hossam S. El-Beltagi:** Writing – review & editing, Validation, Software, Resources, Conceptualization. **Ghulam Murtaza:** Writing – original draft, Supervision, Project administration, Formal analysis, Data curation, Conceptualization. **Muhammad Usman:** Writing – review & editing, Validation, Formal analysis, Data curation, Conceptualization.

Funding

This work was supported by Deanship of Scientific Research, Vice Presidency for Graduate Studies and Scientific Research, King Faisal University, Saudi Arabia (KFU254305). Princess Nourah bint Abdulrahman University Researchers Supporting Project number (PNURSP2026R402), Princess Nourah bint Abdulrahman University, Riyadh, Saudi Arabia.

Declaration of Competing Interest

The authors declare that they have no known competing financial interests or personal relationships that could have appeared to influence the work reported in this paper.

Acknowledgements

This work was supported by Deanship of Scientific Research, Vice Presidency for Graduate Studies and Scientific Research, King Faisal University, Saudi Arabia (KFU254305). Princess Nourah bint Abdulrahman University Researchers Supporting Project number (PNURSP2026R402), Princess Nourah bint Abdulrahman University, Riyadh, Saudi Arabia.

Appendix A. Supporting information

Supplementary data associated with this article can be found in the online version at doi:10.1016/j.indcrop.2025.122390.

Data availability

Data will be made available on request.

References

Abdelslam, O.G., El-khawaga, H.A., 2025. Mitigating salinity stress in two wheat cultivars through Nano-Silicon application: impact on yield and grain composition

Nanosilica particles, Triticum aestivum, yield, silica accumulation. Int. J. Theor. Appl. Res. 4 (1), 563–576.
Angmo, D., Sharma, S.P., Kalia, A., Brar, N.S., Bhardwaj, V., 2023. Effect of cold stress on field performance, chlorophyll fluorescence, electrolyte leakage and leaf gas exchange parameters of potato (*Solanum tuberosum* L.) genotypes. Potato Res. 66 (3), 641–661.
Artekin, A.O., 2022. Economic and political effects of rare earth elements in the new world order. In 27th RSEP ınternational conference on economics, finance & business (pp. 186-204).
Ashesh, A., Purohit, N.N., Paul, R.M., Kaur, S., Singh, A., Kaur, A., Kohli, R., 2025. Current Scenario and Future Prospects. In Colored Cereals. CRC Press, pp. 392–412.
Deng, Z., Wang, J., Yan, Y., Wang, J., Shao, W., Wu, Z., 2025. Biochar-based Bacillus subtilis inoculants promote plant growth: regulating microbial community to improve soil properties. J. Environ. Manag. 373, 123534.
Derdag, S.M., Ouazzani, N., 2025. Advancements in sustainable biochar production from waste: pathways for renewable energy generation and environmental remediation. Biomass 5 (2), 32.
Elbasan, F., Ozfidan-Konakci, C., Yildiztugay, E., Kucukoduk, M., 2020. Rare-earth element scandium improves stomatal regulation and enhances salt and drought stress tolerance by up-regulating antioxidant responses of *Oryza sativa*. Plant Physiol. Biochem. 152, 157–169.
Fan, Y.C., Yuan, Y.Q., Yuan, Y.C., Duan, W.J., Gao, Z.Q., 2025. Research progress on the impact of climate change on wheat production in China. PeerJ 13, e18569.
Fu, Z., Zhang, J., Jiang, J., Wang, W., Zhang, Z., Cao, Q., Liu, X., 2025. Climate change and adaption strategies for wheat-rice rotation production in China. J. Clean. Prod. 518, 145954.
Gentzmann, M.C. (2023). Scandium in Bauxite Residues and other metallurgical by-products (Doctoral dissertation).
Ghosh, A., Mustafiz, A., Pareek, A., Sopory, S.K., Singla-Pareek, S.L., 2022. Glyoxalase III enhances salinity tolerance through reactive oxygen species scavenging and reduced glycation. Physiol. Plant. 174 (3), e13693.
Gómez-Merino, F.C., Gómez-Trejo, L.F., Ruvalcaba-Ramírez, R., Trejo-Téllez, L.I., 2023. Lanthanides as beneficial elements for plants. Benef. Chem. Elem. Plant. Recent Dev. Future Prospects 349–369.
Hafeez, K., Atif, M., Perveen, S., Parveen, A., Akhtar, F., Yasmeen, N., 2024. Unraveling the contribution of copper seed priming in enhancing chromium tolerance in wheat by improving germination, growth, and grain yield. Environ. Sci. Pollut. Res. 31 (27), 39549–39569.
Haider, F.U., Ain, N.U., Siddique, K.H., Farooq, M., Li, Y., 2025. Enhancing bread wheat resilience to cadmium and drought stress: insights from physiological, morphological, and transcriptomic responses to biochar and 24-epibrassinolide application. Biochar 7 (1), 59.
Hamidu, I., Afotey, B., Kwakye-Awuah, B., Annang, D.A., 2025. Synthesis of silica and silicon from rice husk feedstock: A review. Heliyon.
Huang, T., Imran, 2025. Mitigating cadmium contamination in soil using Biochar, sulfur-modified Biochar, and other organic amendments. Int. J. Phytoremediat. 1–14.
Huang, H., Zheng, Y., Wei, D., Yang, G., Peng, X., Fan, L., Zhou, Y., 2022. Efficient removal of pefloxacin from aqueous solution by acid–alkali modified sludge-based biochar: adsorption kinetics, isotherm, thermodynamics, and mechanism. Environ. Sci. Pollut. Res. 29 (28), 43201–43211.
Ikram, M., Minhas, A., Al-Huqail, A.A., Ghoneim, A.M., Mahmood, S., Mahmoud, E., Ali, W., 2024. Promoting tomato resilience: effects of ascorbic acid and sulfur-treated biochar in saline and non-saline cultivation environments. BMC Plant Biol. 24 (1), 1053.
Jabara, M., Wu, J., De Franceschi, S., Manzardo, A., 2025. Assessing mineral and metal resources in life cycle assessment: an overview of existing impact assessment methods. Sustainability 17 (4), 1692.
Jiang, B., Pang, C., Wang, Z., Zhang, S., Wang, S., Zhang, J., Zhou, Q., 2025. Adsorption performance on Thifensulfuron-methyl by novel efficient adsorbent derived from biochar of sugar beet residue. Colloids Surf. A Physicochem. Eng. Asp., 137007
Junior, A.B., Espinosa, D.C.R., Vaughan, J., Tenório, J.A.S., 2021. Recovery of scandium from various sources: a critical review of the state of the art and future prospects. Miner. Eng. 172, 107148.
Kanbar, A., Shakeri, E., Alhajturki, D., Riemann, M., Bunzel, M., Morgano, M.T., Nick, P., 2021. Sweet versus grain sorghum: differential sugar transport and accumulation are linked with vascular bundle architecture. Ind. Crops Prod. 167, 113550.
Kastori, R.R., Putnik-Delić, M.I., Maksimović, I.V., 2023. Rare earth elements application in agriculture. Acta Agric. Serbica 28, 56.
Kaur, P., Mahajan, M., Gambhir, H., Khan, A., Khan, M.I.R., 2024. Rare earth metallic elements in plants: assessing benefits, risks and mitigating strategies. Plant Cell Rep. 43 (9), 216.
Kumar, A., Bhattacharya, T., Shaikh, W.A., Chakraborty, S., Sarkar, D., Biswas, J.K., 2022a. Biochar modification methods for augmenting sorption of contaminants. Curr. Pollut. Rep. 8 (4), 519–555.
Kumar, S.S., Wani, O.A., Malik, A.R., Kumar, S., Patel, R., 2025. Biochar for Food Security and Environmental Sustainability Under Current Climate Change Scenario. In Agricultural Diversification for Sustainable Food Production. Springer Nature Singapore, Singapore, pp. 59–88.
Kumar, S., Yadav, A., Verma, R., Dubey, A.K., Narayan, S., Pandey, A., Sanyal, I., 2022b. Metallothionein (MT1): a molecular stress marker in chickpea enhances drought and heavy metal stress adaptive efficacy in transgenic plants. Environ. Exp. Bot. 199, 104871.
Laus, M.N., Blando, F., Soccio, M., 2023. Glyoxalase I assay as a possible tool for evaluation of biological activity of antioxidant-rich plant extracts. plants 12 (5), 1150.
Li, Y., Xu, X., Suo, L., Sun, Y., Sun, N., Liu, J., Liao, S., 2023. The effects of calcium and sulfur fertilizers accompanied by different side elements on the growth and Cd uptake of Spinacia oleracea grown in cd-contaminated alkaline soil. Horticulturae 9 (7), 835.
Lin, N., Luo, X., Wen, J., Fu, J., Zhang, H., Siddique, K.H.M., Zhao, Y., 2024. Black biodegradable mulching increases grain yield and net return while decreasing carbon footprint in rain-fed conditions of the Loess Plateau. Field Crops Res. 318, 109590. https://doi.org/10.1016/j.fcr.2024.109590.
Liu, S., Fan, H.R., Santosh, M., Liu, X., Wang, Q.W., Butcher, A.R., 2023. Geological resources of scandium: a review from a Chinese perspective. Int. Geol. Rev. 65 (19), 3065–3086.
Liu, S., Pu, S., Deng, D., Huang, H., Yan, C., Ma, H., Razavi, B.S., 2020. Comparable effects of manure and its biochar on reducing soil Cr bioavailability and narrowing the rhizosphere extent of enzyme activities. Environ. Int. 134, 105277. https://doi.org/10.1016/j.envint.2019.105277.
Lu, Y., Wang, Q., Yu, F., Zhang, S., Zhu, X., 2023. Carbothermal reduction synthesis of sulfide-modified biochar for heavy metal removal. Carbon Res. 2 (1), 5.
Lyu, H., Xia, S., Tang, J., Zhang, Y., Gao, B., Shen, B., 2020. Thiol-modified biochar synthesized by a facile ball-milling method for enhanced sorption of inorganic Hg^{2+} and organic CH_3Hg^+. J. Hazard. Mater. 384, 121357.
Maham, M., Rabia, C., Anum, I., Ahad, I.U., 2025. Critical and strategic raw materials for energy storage devices. Batteries 11 (4), 163.
Mahey, S., Kumar, R., Sharma, M., Kumar, V., Bhardwaj, R., 2020. A critical review on toxicity of cobalt and its bioremediation strategies. SN Appl. Sci. 2 (7), 1279.
Murmu, K., Sarkar, A., Sarma, S.S., Jana, K., Murmu, S., 2025. Mitigating the impact of drought and heat stress on crop productivity and environmental sustainability. Drought Heat. Stress Agric. 155–173.
Murtaza, G., Ahmed, Z., Iqbal, R., Deng, G., 2025c. Biochar from agricultural waste as a strategic resource for promotion of crop growth and nutrient cycling of soil under drought and salinity stress conditions: a comprehensive review with context of climate change. J. Plant Nutr. 1–52.
Murtaza, G., Ahmed, Z., Valipour, M., Ali, I., Usman, M., Iqbal, R., Tariq, A., 2024b. Recent trends and economic significance of modified/functionalized biochars for remediation of environmental pollutants. Sci. Rep. 14 (1), 217.
Murtaza, G., Hassan, N.E., Usman, M., Deng, G., Ahmed, Z., Iqbal, J., Lackner, M., 2025a. Synergistic effects of allantoin and *Achyranthes japonica*-biochar profoundly alleviate lead toxicity during barley growth. Ecotoxicol. Environ. Saf. 290, 117784.
Murtaza, G., Usman, M., Ahmed, Z., Hyder, S., Alwahibi, M.S., Rizwana, H., Zeng, Y., 2024a. Improving wheat physio-biochemical attributes in ciprofloxacin-polluted saline soil using nZVI-modified biochar. Ecotoxicol. Environ. Saf. 286, 117202.
Murtaza, G., Usman, M., Ahmed, Z., Alwahibi, M.S., Rizwana, H., Iqbal, J., Deng, G., 2025b. Fe-modified biochar improves tobacco productivity by promoting root growth, plant biochemical traits and nicotine level: a three years field study. J. Soil Sci. Plant Nutr. 1–17.
Naqash, N., Yadav, K.K., Shaik, A.S., Alam, M.W., Djajadi, D., Sunarto, D.A., Wani, A.K., 2025. Microplastic pollution in terrestrial systems: sources and implications for soil functioning and plant performance. Water Air Soil Pollut. 236 (3), 172.
Pan, G., Geng, S., Wang, L., Xing, J., Fan, G., Gao, Y., Zhang, Z., 2025. Effects of Modified Biochar on Growth, Yield, and Quality of *Brassica chinensis* L. in Cadmium Contaminated Soils. Plants 14 (4), 524.
Peng, Y., Su, L., Liu, M., Zeng, C., Xiang, B., Xie, Z., Zhou, N., 2025. Biochar-enhanced sulfur: mechanistic insights into a novel and effective bactericide. Nanomaterials 15 (9), 697.
Qin, S., Zhang, Y., Wang, J., Wang, C., Mo, Y., Gong, S., Zhang, B., 2024. Response of leaf gas exchange parameters to mulching materials in wheat field was mediated by stomatal morphology and ABA content. J. Plant Growth Regul. 43 (6), 1985–1998.
Qu, J., Che, N., Niu, G., Liu, L., Li, C., Liu, Y., 2023. Iron/manganese binary metal oxide-biochar nano-composites with high adsorption capacities of Cd^{2+}: preparation and adsorption mechanisms. J. Water Process Eng. 51, 103332.
Raza, A., Khare, T., Zhang, X., Rahman, M.M., Hussain, M., Gill, S.S., Varshney, R.K., 2025. Novel strategies for designing climate-smart crops to ensure sustainable agriculture and future food security. J. Sustain. Agric. Environ. 4 (2), e70048.
Ren, T., Chen, N., Mahari, W.A.W., Xu, C., Feng, H., Ji, X., Lam, S.S., 2021. Biochar for cadmium pollution mitigation and stress resistance in tobacco growth. Environ. Res. 192, 110273.
Sana, Aqeel, U., Aftab, T., Gill, R., Gill, S.S., Naeem, M., 2025. Harnessing gasotransmitters for enhanced plant resilience: strategies for managing metalloid (s) stress. J. Plant Growth Regul. 1–24.
Santos, D.C., Evaristo, R.B., Dutra, R.C., Suarez, P.A., Silveira, E.A., Ghesti, G.F., 2025. Advancing biochar applications: a review of production processes, analytical methods, decision criteria, and pathways for scalability and certification. Sustainability 17 (6), 2685.
Sharma, S., Singh, G., Wang, Y., White, J.C., Xing, B., Dhankher, O.P., 2023. Nanoscale sulfur alleviates silver nanoparticle toxicity and improves seed and oil yield in Soybean (*Glycine max*). Environ. Pollut. 336, 122423.
Shtangeeva, I., 2022. Accumulation of scandium, cerium, europium, hafnium, and tantalum in oats and barley grown in soils that differ in their characteristics and level of contamination. Environ. Sci. Pollut. Res. 29 (27), 40839–40853.
Singh, A., Sharma, R., Singh, S., Singh, R.K., Alexiou, A., Sousa, J.R., Ghazaryan, K., 2025. Addressing abiotic stresses and advancing SDGs by biochar for sustainable agriculture and environmental restoration. Egypt. J. Soil Sci. 65 (1), 463–489.
Sonawane, R., Kandasubramanian, B., 2025. Harnessing functionalized biochar for enhanced electrochemical properties in secondary batteries. J. Electron. Mater. 1–17.

Soni, P., Shivhare, R., Kaur, A., Bansal, S., Sonah, H., Deshmukh, R., Ram, H., 2021. Reference gene identification for gene expression analysis in rice under different metal stress. J. Biotechnol. 332, 83–93.
Syarifuddin, S., Suryani, S., Tahir, D., 2025. Global advances and innovations in bacteria-based biosorption for heavy metal remediation: a bibliometric and analytical perspective. Integr. Environ. Assess. Manag. 21 (3), 507–525.
Tiwari, M., Rathod, T., Bhangare, R., Sahu, S.K., Pulhani, V., 2025. Comprehensive elemental and carbon profiling of Punjab's soils: distribution patterns, pollution assessment, and source attribution. Environ. Geochem. Health 47 (5), 1–19.
Tomczuk, M., Godlewska-Żyłkiewicz, B., Bajguz, A., 2025. Gadolinium in the environment: a double-edged sword for plant growth and ecosystem stability. Metabolites 15 (6), 415.
Umaru, K.I., Terungwa, J.I., Umaru, I.J., 2025. Sorption Studies of Biochar-Based Composites for Removal of Organic Contaminants. Biochar-based Composites: Preparation, Characterization and Applications. Springer Nature Singapore, Singapore, pp. 235–256.
Upadhyay, R.K., 2025. Metallic Minerals and Their Deposits. In Geology and Mineral Resources. Springer Nature Singapore, Singapore, pp. 495–561.
Varkolu, M., Gundekari, S., Palla, V.C.S., Kumar, P., Bhattacharjee, S., Vinodkumar, T., 2025. Recent advances in Biochar production, characterization, and environmental applications. Catalysts 15 (3), 243.
Vijaya, Idrishi, R., Singh, S., Islam, M., 2025. Processing of Rice Husk and Its Applications. In Rice Husk Biomass: Processing. Properties and Applications. Springer Nature Singapore, Singapore, pp. 1–26.
Wang, Z., Li, M.Y.H., Liu, Z.R.R., Zhou, M.F., 2021. Scandium: ore deposits, the pivotal role of magmatic enrichment and future exploration. Ore Geol. Rev. 128, 103906.
Wang, Y., Yu, T., Wang, C., Wei, J., Zhang, S., Liu, Y., Xu, Z., 2023. Heat shock protein TaHSP17.4, a TaHOP interactor in wheat, improves plant stress tolerance. Int. J. Biol. Macromol. 246, 125694.
Wang, S., Zhang, T., Jahan, I., Zhou, Y., Li, S., Cai, Y., Cai, K., 2025. Si-modified biochar mediated tomato resistance to bacterial wilt by increasing soil silicon availability and inducing plant defense. Plant Physiol. Biochem., 110163
Wiche, O., Dittrich, C., Pourret, O., Monei, N., Heim, J., Lambers, H., 2023. Relationships between carboxylate-based nutrient-acquisition strategies, phosphorus-nutritional status and rare earth element accumulation in plants. Plant Soil 489 (1), 645–666.
Williams, J.H., Gbadomosi, M., Greytak, A.B., Myrick, M.L., 2023. Measuring the surface area of carbon black using BET isotherms: an experiment in physical chemistry. J. Chem. Educ. 100 (12), 4838–4844.
Wu, Z., Gu, X., Zha, L., Yang, Q., Zhou, Y., Zeng, Z., 2024. Structural and functional insights into yeast Tbf1 as an atypical telomeric repeat-binding factor. Structure 32 (7), 889–898.e3.
Xiao, C., Yang, H., Chen, X., Li, J., Cai, X., Long, J., 2024. Application of lanthanum at the heading stage effectively suppresses cadmium accumulation in wheat grains by downregulating the expression of tazip7 to increase cadmium retention in nodes. Plants 13 (20), 2921.
Xiong, X., Liu, J., Xiao, T., Lin, K., Huang, Y., Deng, P., Wang, J., 2025. Remediation of uranium-contaminated water and soil by biochar-based materials: a review. Biochar 7 (1), 41.
Xu, Y., Li, Y., Wang, P., Feng, C., Cao, S., Li, J., 2025. Unraveling the geochemical behaviors of rare earth elements (REEs) in Chinese drinking natural mineral waters: Environmental and health perspectives. J. Hazard. Mater., 138731
Yan, X., Wang, Z., Zhao, M., Hao, J., Liu, J., Yan, Y., Ge, G., 2024. Hydrothermal biochar enhances the photosynthetic efficiency and yield of alfalfa by optimizing soil chemical properties and stimulating the activity of microbial communities. Sci. Rep. 14 (1), 31420.
Yang, X., Luo, S., Zhou, J., Sun, P., Guo, Y., Zhao, J., Gao, B., 2025. Ball-milled dysprosium oxide loaded biochar-montmorillonite composite for efficient removal and great recycling performance of cationic organic pollutants. Ind. Crops Prod. 235, 121777.
Yang, X., Wang, J., Xia, X., Zhang, Z., He, J., Nong, B., Luo, T., Feng, R., Wu, Y., Pan, Y., Xiong, F., Zeng, Y., Chen, C., Guo, H., Xu, Z., Li, D., Deng, G., 2021. OsTTG1, a WD40 repeat gene, regulates anthocyanin biosynthesis in rice. Plant journal cell molecular biology 107 (1), 198–214.
Zadokar, A., Negi, S., Kumar, P., Bhargava, B., Sharma, R., Irfan, M., 2023. Molecular insights into rare earth element (REE)-mediated phytotoxicity and its impact on human health. Environ. Sci. Pollut. Res. 30 (36), 84829–84849.
Zaman, W., Ayaz, A., Park, S., 2025. Nanomaterials in agriculture: A pathway to enhanced plant growth and abiotic stress resistance. Plants 14 (5), 716.
Zhang, L., Luo, M., Jiang, X., Tao, Y., Yang, D., Wang, L., Zang, L., 2025. Comprehensive assessment of biochar remediation performance for cadmium-contaminated sediment as affected by multiple physicochemical factors. J. Environ. Chem. Eng. 13 (3), 116228.
Zhao, B., O'Connor, D., Shen, Z., Tsang, D.C., Rinklebe, J., Hou, D., 2020. Sulfur-modified biochar as a soil amendment to stabilize mercury pollution: An accelerated simulation of long-term aging effects. Environ. Pollut. 264, 114687.
Zheng, M., Zhang, J., Wang, P., Jin, H., Zheng, Y., Qiao, S.Z., 2024. Recent advances in electrocatalytic hydrogenation reactions on copper-based catalysts. Adv. Mater. 36 (14), 2307913.
Zhu, H., Ma, H., Xu, L., Yu, D., Zhong, S., Chen, Y., Pu, S., 2025. The regulatory role of dissolved oxygen in N-doped biochar-driven nonradical oxidation. Chem. Eng. J. 520, 165915. https://doi.org/10.1016/j.cej.2025.165915.